



Fair Isle Harbour Improvement Works

A.12 Wave Modelling

On behalf of **Shetland Isle Council (SIC)**



Project Ref: 11168 | Rev: Version 1.0 | Date: April 2023

Registered Office: Buckingham Court Kingsmead Business Park, London Road, High Wycombe, Buckinghamshire, HP11 1JU
Office Address: 10 Queen Square, Bristol, BS1 4NT
T: +44 (0)117 332 7840 E: bristol@stantec.com



Fair Isle Wave Modelling

March 2023

This page left intentionally blank for pagination.

Mott MacDonald
Ground floor
Royal Liver Building
Pier Head
Liverpool L3 1JH
United Kingdom

T +44 (0)151 482 9910
mottmac.com

Fair Isle Wave Modelling

March 2023

Issue and Revision Record

Revision	Date	Originator	Checker	Approver	Description
01	27/1/23	NDED	JW		Draft
02	14/3/23	NDED	RC		Final

Document reference: | | 02 |

Information class: Standard

This document is issued for the party which commissioned it and for specific purposes connected with the above-captioned project only. It should not be relied upon by any other party or used for any other purpose.

We accept no responsibility for the consequences of this document being relied upon by any other party, or being used for any other purpose, or containing any error or omission which is due to an error or omission in data supplied to us by other parties.

This document contains confidential information and proprietary intellectual property. It should not be shown to other parties without consent from us and from the party which commissioned it.

Contents

Executive summary	1
1 Introduction	3
1.1 Background	3
1.2 Report structure	3
2 Data and methodology	5
2.1 Bathymetric data	5
2.2 Datums	5
2.3 Waves	5
2.3.1 Wave parameters definition	5
2.3.2 Wave data	5
2.4 Wind data	6
2.5 Water level data	7
2.6 Proposed layout	8
2.7 Methodology	9
3 Regional MIKE21 FM SW model	11
3.1 Model forcing by wind and water levels	12
3.2 Model Boundary	12
3.3 Regional model set up	12
3.4 Regional model calibration	14
3.5 Regional model validation	17
4 Extreme value analysis	19
4.1 EVA of Hs	19
4.1 Tp and Hs relationship	21
4.2 Wind Speed and Hs relationship	21
4.3 Extreme wave conditions	25
5 Local MIKE21 FMSW model	26
5.1 Fair Isle local model domain	26
5.2 Fair Isle model set up	27
6 Results	30
6.1 AEP results	30
6.2 Wave climate results	33
6.3 Annual wave occurrences	34

Appendices	39
A. Comparison of regional and local models	40
B. Wave occurrence	41
B.1 Baseline	41
B.2 Layout 01	44

Tables

Table 2.1: Tidal levels at Fair Isle	8
Table 3.1: Summary of MIKE21 FMSW regional model setup	13
Table 3.2: Statistics of the comparison between measured wave height and zero-crossing wave period against modelled wave height.	16
Table 3.3: Performance measured of the comparison between measured wave height and zero-crossing wave period at Lerwick against modelled wave height and zero-crossing wave period.	16
Table 3.4: Statistics of the comparison between measured wave height	18
Table 3.5: Performance measured of the comparison between measured wave height at Lerwick against modelled wave height for the validation period.	18
Table 4.1: Summary of the wave and wind conditions for the local wave model simulations for each AEP event.	25
Table 5.1: Summary of MIKE21 FMSW local model set up	27
Table 6.1: AEP results at extraction points (Fa1, Fa2, Fa3, Fa4 and Fa5) for the existing and 'Layout 01' for the high Hs.	31
Table 6.2: AEP results at Fa1, Fa2 and Fa3 (extraction points behind the breakwater) for the baseline and 'Layout 01' for the high Tp.	32
Table 6.3: Annual mean wave conditions at the five extraction points for the baseline and 'Layout 01'.	33
Table 6.4: High Hs conditions at the five extraction points for the baseline and 'Layout 01'.	33
Table 6.5: High Tp conditions at Fa1, Fa2 and Fa3 for the baseline and 'Layout 01'.	33
Table 6.6: Annual wave occurrence of Hs (m) against Tp (s) at Fa3 for the baseline.	34
Table 6.7: Annual wave occurrence of Hs (m) against Tp (s) at Fa3 for 'Layout 01'.	34

Figures

Figure 1.1: Location of Fair Isle and location of extraction points.	2
Figure 1.1: Location of the 'North Haven' Ferry Terminal at Fair Isle.	3
Figure 2.1: Location of ERA-5 extraction location (blue dashed rectangle) and Lerwick buoy (red dot). Fair Isle is highlighted in the red square.	6
Figure 2.2: Wind speed distribution map during a storm on 5 November 1985, 12:00 UTC.	6
Figure 2.3: Location of: (a) Sumburgh (blue dot); (b) Fair Isle (green dot) tide stations; and (c) location of the Lerwick buoy (red dot).	7

Figure 2.4: Predicted water level at Sumburgh (1979 to 2020).	8
Figure 2.5: Predicted water level at Fair Isle (1979 to 2020).	8
Figure 2.6: Outline design for the proposed 'Layout 01' ferry terminal at Fair Isle.	9
Figure 2.7: Methodology followed in the present study.	10
Figure 3.1: MIKE21 FM SW regional model domain and bathymetry of: (a) the whole regional model; and (b) enlarged view at the Fair Isle model domain boundaries indicated as the red lines.	11
Figure 3.2: MIKE21 FM SW regional model domain mesh of: (a) the whole regional model; and (b) enlarged view at the Fair Isle model domain boundaries indicated as the red lines.	12
Figure 3.3: Comparison of measured and hindcast wind speed and direction at Sumburgh Airport (Figure 3.1b).	14
Figure 3.4: Time series plots showing historical measured waves (blue cross) at Lerwick and regional modelled (red line) data for (a) significant wave height, H_s; and (b) zero-crossing wave period, T_z for the calibration period (3 March to 31 May 1985).	15
Figure 3.5: Scatter plot comparison between: (a) measured wave height, H_s; and (b) zero-crossing wave period, T_z, at Lerwick against modelled regional results.	15
Figure 3.6: Significant wave height (H_s) predicted by the regional MIKE21 FM SW model during the storm's peak on 20 April 1985 at 23:00 UTC.	17
Figure 3.7: Time series plots showing historical measured waves (blue cross) at Lerwick and regional modelled (red line) data for the significant wave height, H_s, for the validation period (5 October to 7 November 1985).	17
Figure 3.8: Scatter plot comparison between measured wave height and at Lerwick against modelled regional results.	17
Figure 4.1: Location of waves data extraction at FI 4, FIE, FI3, FID, FI2, FIC, FI1 and FIB with the filtered H_s rose plot based on the selected dominant directional sector.	20
Figure 4.2: Probability distribution fit of H_s at the eight dominant directional sectors (N, NE, E, SE, E, SW, W, NW)	22
Figure 4.3: Relationship between T_p and H_s at the directional sectors (N, NE, E, SE, E, SW, W, NW) with the 100% AEP (1:1 year RP) of H_s .	23
Figure 4.4: Relationship between wind speed and H_s at the directional sectors (N, NE, E, SE, E, SW, W, NW).	24
Figure 5.1: Local model bathymetry and mesh of: (a) the whole local model domain with open boundary locations indicated as the red lines; and (b) an enlarged view of the existing breakwater at the project site.	26
Figure 5.2: Enlarged view of mesh and bathymetry of the proposed 'Layout 01' with data extraction location points (Fa1, Fa2, Fa3, Fa4 and Fa5) to assess wave conditions.	27
Figure 5.3: Location of Point 1 and H_s time series from the regional and local wave models.	29
Figure 6.1: Wave rose plots at Fa1, Fa2 Fa3, Fa4 and Fa5 for H_s (m) against MWD (deg.N) (a1-a5) and T_p (s) against MWD (deg.N) (b1-b5) for the baseline conditions.	36
Figure 6.2: Wave rose plots at Fa1, Fa2 Fa3, Fa4 and Fa5 for H_s (m) against MWD (deg.N) (a1-a5) and T_p (s) against MWD (deg.N) (b1-b5) for the 'Layout 01' conditions.	37

Tables – Appendices

Table B.1: Annual wave occurrence of Hs (m) against Tp (s) at Fa1 for the baseline.	41
Table B.2: Annual wave occurrence of Hs (m) against Tp (s) at Fa2 for the baseline.	41
Table B.3: Annual wave occurrence of Hs (m) against Tp (s) at Fa4 for the baseline.	42
Table B.4: Annual wave occurrence of Hs (m) against Tp (s) at Fa5 for the baseline.	43
Table B.5: Annual wave occurrence of Hs (m) against Tp (s) at Fa1 for the 'Layout 01'.	44
Table B.6: Annual wave occurrence of Hs (m) against Tp (s) at Fa2 for the 'Layout 01'.	44
Table B.7: Annual wave occurrence of Hs (m) against Tp (s) at Fa4 for the 'Layout 01'.	45
Table B.8: Annual wave occurrence of Hs (m) against Tp (s) at Fa5 for the 'Layout 01'.	46

Figures – Appendices

Figure A.1: Time series of Hs based on the regional and local results at Point 2.	40
Figure A.2: Time series of Hs based on the regional and local results at Point 3.	40

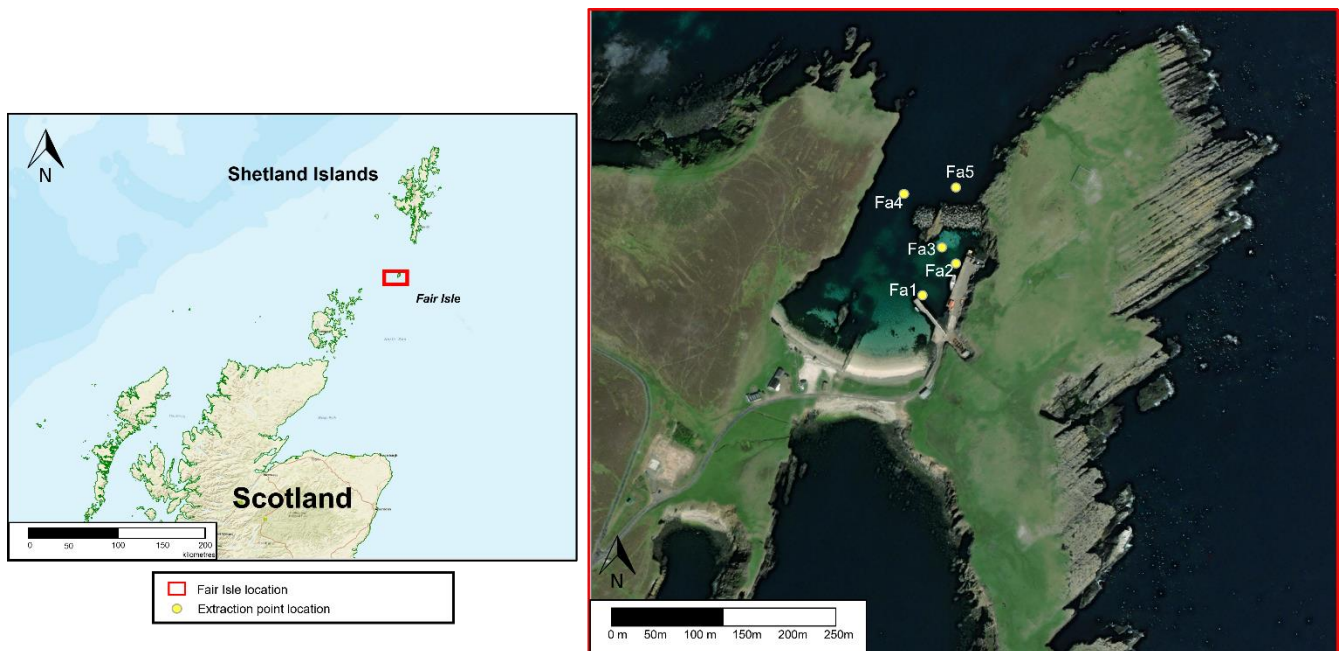
Executive summary

Mott MacDonald Ltd is working with Shetland Island Council (SIC) and ZetTrans, owner of the Fair Isle (North Haven) Ferry Terminal, to develop an Outline Business Case (OBC) for upgrade works to the existing ferry terminal at 'North Haven' located on Fair Isle, 24 miles off the southern tip of the Shetland Islands, Scotland.

The project aims to upgrade the current ferry terminal to accommodate different vessels, facilitate access, and provide improved shelter from wave action. In support of the project, numerical wave modelling works are needed to simulate wave climate at 'North Haven' and to calculate the extreme waves that could be present during the lifetime of the new terminal.

In the present study, a regional two-dimensional (2D) spectral wave model (MIKE21 FMSW) has been built, calibrated, and validated against historical wave data at Lerwick station. To represent correctly the propagation of waves from offshore to nearshore, the regional model covers the Shetland Islands and all relevant coastal and offshore areas that influence the wave climate. The model calibration and validation conformed to robust model performance metrics (Williams and Esteves, 2017) during normal wave conditions and storm events. The regional model was judged suitable for defining offshore boundary conditions for the local wave model. The regional model was run for 42 years (January 1979 to December 2020). Extreme wave analysis of these data was used to define wave characteristics with 100%, 50%, 10%, and 1% Annual Exceedance Probability (AEP).

Using a local MIKE21 FMSW wave model, these extreme events were transformed into the study area based on the regional model results. Although calibration of the local model was not performed due to the absence of measured local data, the model was validated using the regional model. The local wave model was run for baseline (current infrastructure) and the new proposed layout ('Layout 01') for each AEP event. It was also run from January to December 2018 to provide annual wave conditions. The year 2018 was selected as it included the highest wave height from the 42-year regional wave model results. Wave data from the local model were extracted and analysed at 5 locations (Figure 1.1) along the frontage of the ferry terminal to define the wave conditions required for assessment and design purposes.

Figure 1.1: Location of Fair Isle and location of extraction points.

Source: Mott MacDonald, 2023

Results from the local wave model showed that:

- H_s slightly decreased at Fa1, Fa2 and Fa3 for Layout 01 due to shelter behind the breakwater;
- High T_p values were predicted at Fa1, Fa2 and Fa3 in Layout 01 due to reflection and directional spreading;
- The dominant wave direction is northwest to the north at Fa4 and Fa5 for the baseline layout. At these locations, the breakwater provides no shelter. At Fa2 and Fa3, behind the existing breakwater, the dominant direction is southwest to the west. Due to wave reflection, Fa1 shares the same dominant wave direction as Fa4 and Fa5; and
- The dominant wave direction for 'Layout 01' conditions varies slightly from the baseline case at Fa2 and Fa3. At these locations, waves from the north are marginally more dominant due to the shape of the proposed layout.

It should be noted that the local wave model was not calibrated; therefore, there will always be some uncertainty until model calibration is performed. Nevertheless, the present study provides a useful guide to the performance of Layout 01 concerning impacts on the local wave climate.

It is important to note that the information from this study should not be used to assist in designing the ferry terminal infrastructure. If the project were to be taken forward, the following work is recommended to:

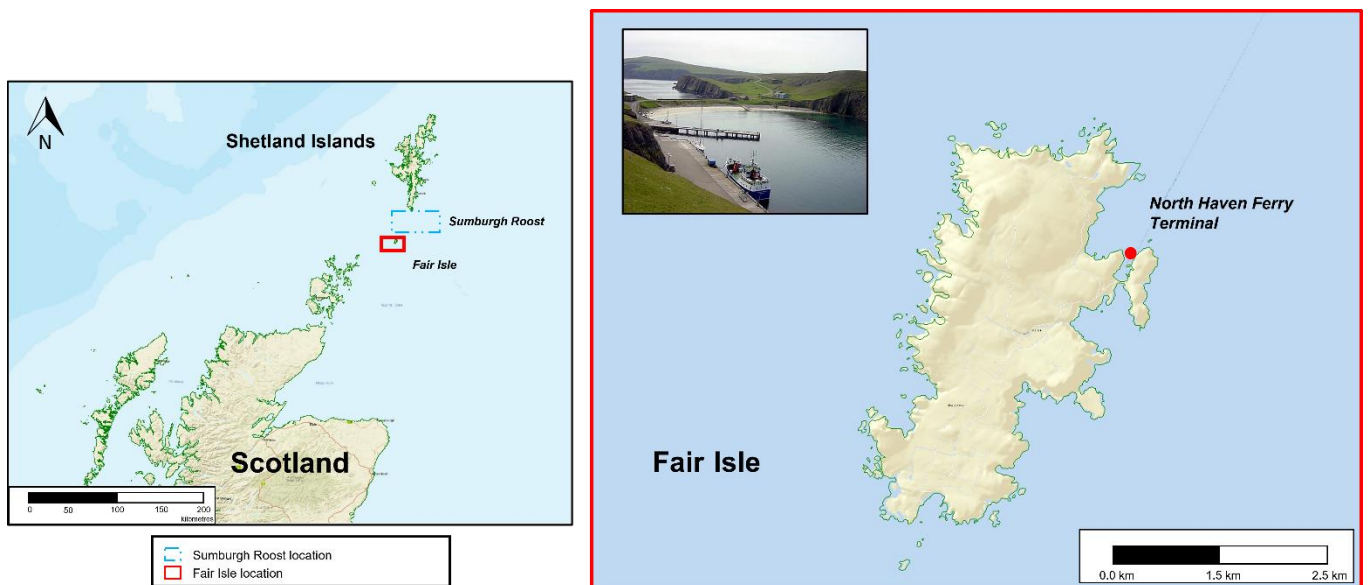
- Acquire local wave and wind data to enable calibration of the local wave model; and
- Use a model like MIKE3 Wave FM for design purposes that includes more physically realistic representations of reflection, diffraction and wave-wave interactions.

1 Introduction

1.1 Background

Mott MacDonald Ltd is working with Shetland Island Council (SIC) and ZetTrans, owner of the Fair Isle (North Haven) Ferry Terminal, to develop an Outline Business Case (OBC) for upgrade works to the existing ferry terminal at ‘North Haven’ located on Fair Isle, 24 miles off the southern tip of the Shetland Islands, Scotland, (Figure 1.1). The island is separated from Shetland by Sumburgh Roost (Figure 1.1 and Figure 2.1b), where two tidal streams meet to create one of the most demanding stretches of water in the United Kingdom.

Figure 1.1: Location of the ‘North Haven’ Ferry Terminal at Fair Isle.



Source: Mott MacDonald, 2023

Since the existing terminal is approaching the end of its life and does not meet modern standards, the Fair Isle Ferry Replacement Project (‘the project’) aims to accommodate different vessels, facilitate access, and provide improved shelter from wave action. In support of the OBC, an analysis of the wave climate is required to assess the project’s exposure to local wind-generated waves and swell from several directions. By establishing a local wave model, the efficacy of the harbour designs can be assessed.

Wave modelling has been undertaken using MIKE21 Flexible Mesh (FM) Spectral Wave (SW) software. Models have been developed at regional and local scales to simulate swell and wind wave propagation from offshore to the ferry terminal. Results extracted from the model have been analysed to characterise the extreme wave conditions for different annual exceedance probabilities (AEP) and to establish a representative annual wave climate in the harbour.

1.2 Report structure

The report presents the key wave modelling activities, data and results. It is structured as follows:

- Section 2: outlines the numerical modelling approach and describes the bathymetric, wave, wind and water level data used to build the regional and local wave models. It also includes a description of the proposed new ferry layout;
- Section 3: describes the regional wave model built, validation and calibration;
- Section 4: presents an extreme value analysis (EVA) used to define the characteristics of 100%, 50%, 10% and 1% Annual Exceedance Probability (AEP) of wave and wind events;
- Section 5: describes the local wave model domain, set-up, and model runs;
- Section 6: presents and discusses the local wave model results; and
- Section 7: summarises the wave modelling work.

2 Data and methodology

The data inputs for the modelling study included open-source data and site-specific measurements. It is noted that the model outputs from this study rely heavily on the accuracy of the dataset used; thus, they were quality assured before use.

2.1 Bathymetric data

The bathymetric data used to build wave models comprised:

- UK Hydrographic Office (UKHO)¹ charts;
- European Marine Observation and Data Network (EMODnet, 2020)²;
- A bespoke bathymetry survey of Fair Isle, provided by Aspect Ltd in June 2022.

As any model's performance is closely related to the accuracy of the bathymetry/topography data used to build the model, care was taken to ensure that the natural features were represented accurately within the constraints imposed by the data available for the study. The regional and local model was entirely built on freely available data from UKHO and EMODnet, prioritising the UKHO data and local bathymetry due to the better spatial and temporal resolution associated with these data.

2.2 Datums

Geographical data used in this study is referenced to a horizontal datum defined by geographical coordinates (longitude/latitude). The vertical datum is referenced to the mean sea level (MSL) for the regional wave model and Ordnance Datum Newlyn (mODN) for the local wave model.

2.3 Waves

2.3.1 Wave parameters definition

Wave parameters used in this report are defined as:

- **Significant wave height:** The significant wave height, H_s (m), is the mean of the highest third of the waves in a time series of waves representing a particular sea state. This corresponds well with the average height of the highest waves in a wave group;
- **Peak wave period:** The peak wave period, T_p (s), is the wave period with the highest energy. The analysis of the distribution of the wave energy as a function of wave frequency ($1/\text{period}$) for a time series of individual waves is referred to as a spectral analysis; and
- **Mean wave direction:** The mean wave direction, MWD (expressed as degrees from north), is defined as the mean of all the individual wave directions in a time series representing a particular sea state.

2.3.2 Wave data

Modelled wave data quantifying H_s , T_p and MWD were available for the study and included:

- Hourly model hindcast wave data from 1979 to 2020 (42 years) from The European Centre for Medium-Range Weather Forecasts (ECMWF) ERA5 dataset with a 0.5-degree spatial

¹ [Bathymetry data Service \(admiralty.co.uk\)](https://www.admiralty.co.uk)

² <https://portal.emodnet-bathymetry.eu/>

resolution. This dataset was used as offshore boundary conditions in the regional wave model and was extracted at the grid location shown in Figure 2.1; and

- Historical measured wave data at Lerwick (Figure 2.1), quantifying H_s and zero-crossing wave period (T_z), were obtained from Cefas database³. MWD data were not available. The H_s and T_z data were used to calibrate the regional model (Section 3.4).

Figure 2.1: Location of ERA-5 extraction location (blue dashed rectangle) and Lerwick buoy (red dot). Fair Isle is highlighted in the red square.

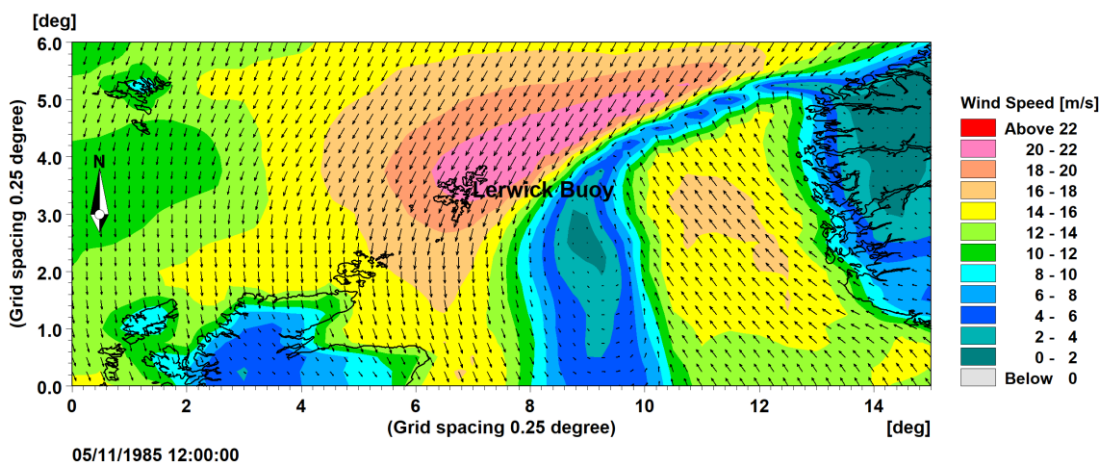


Source: Mott MacDonald, 2023

2.4 Wind data

As the wind is the primary forcing contribution to ocean wave formation, acquiring and using accurate wind data is important in wave modelling studies. This study used wind data from the ECMWF ERA5⁴ database (0.25-degree spatial resolution, 1-hr intervals). A 42-year record of U and V wind components at an elevation of 10m was extracted from the database from January 1979 to December 2020. Figure 2.2 shows an example of a spatial wind map during a storm. The Lerwick buoy recorded the maximum H_s on 5 November 1985 at 12:00 UTC. Around this time, the figure shows strong winds at Lerwick up to 22 m/s from the northeast.

Figure 2.2: Wind speed distribution map during a storm on 5 November 1985, 12:00 UTC.



Source: Mott MacDonald, 2023 with ECMWF ERA5 data

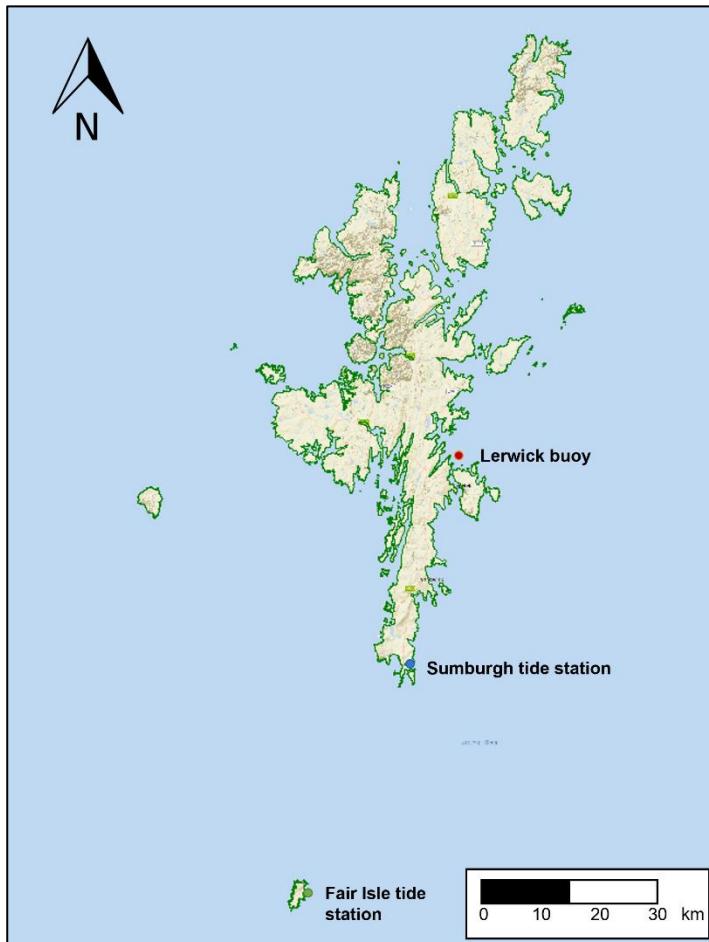
³ <http://wavenet.cefas.co.uk/Map?ZoomTo=0.4755%2C53.0582>

⁴ <https://www.ecmwf.int/en/forecasts/datasets/reanalysis-datasets/era5>

2.5 Water level data

Without any locally measured tidal data for the regional wave model runs, predicted water level data at Sumburgh (Figure 2.3) were extracted from Delft Dashboard⁵. Figure 2.4. shows the 42-year time series (1979 to 2020) of the predicted water level at Sumburgh. Tidal characteristics at Fair Isle extracted from the Admiralty TotalTide⁶ are shown in Table 2.1. This table shows spring and neap tide ranges are 1.6m and 0.7m, respectively.

Figure 2.3: Location of: (a) Sumburgh (blue dot); (b) Fair Isle (green dot) tide stations; and (c) location of the Lerwick buoy (red dot).

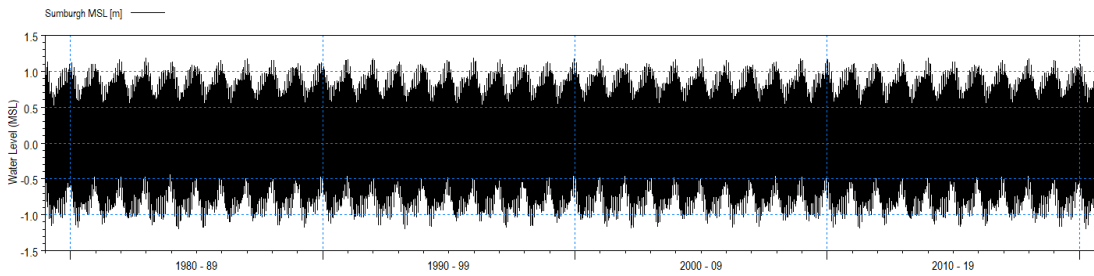


Source: Mott MacDonald, 2023

⁵ [Delft Dashboard - Delft Dashboard - Deltares Public Wiki](#)

⁶ <https://www.admiralty.co.uk/>

Figure 2.4: Predicted water level at Sumburgh (1979 to 2020).



Source: Mott MacDonald, 2023. Contains Delft data, 2022

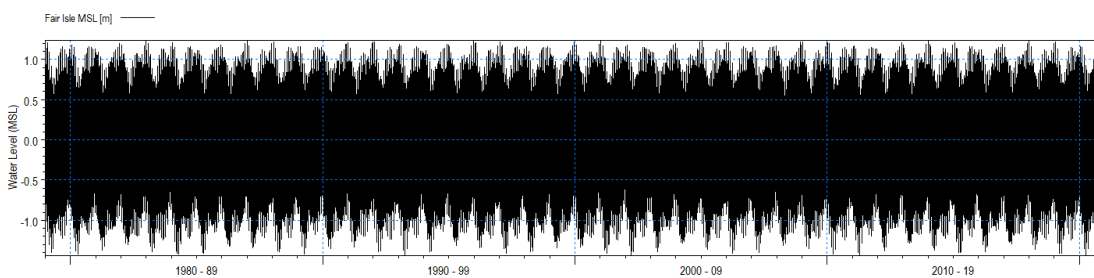
Table 2.1: Tidal levels at Fair Isle

Tidal level	Chart datum (mCD)	Ordnance datum Newlyn (mODN)
Highest Astronomical Tide (HAT)	2.70	1.78
Mean High Water Springs (MHWS)	2.20	1.28
Mean High Water Neaps (MHWN)	1.70	0.78
Mean Sea Level (MSL)	1.37	0.45
Mean Low Water Neaps (MLSN)	1.00	0.08
Mean Low Water Springs (MLWS)	0.60	-0.32
Lowest Astronomical Tide (LAT)	2.70	1.78

Source: Admiralty Total Tide, 2021

For the local model, predicted water level data at Fair Isle (Figure 2.3) were also extracted from Delft Dashboard from 1979 to 2020 (Figure 2.5).

Figure 2.5: Predicted water level at Fair Isle (1979 to 2020).

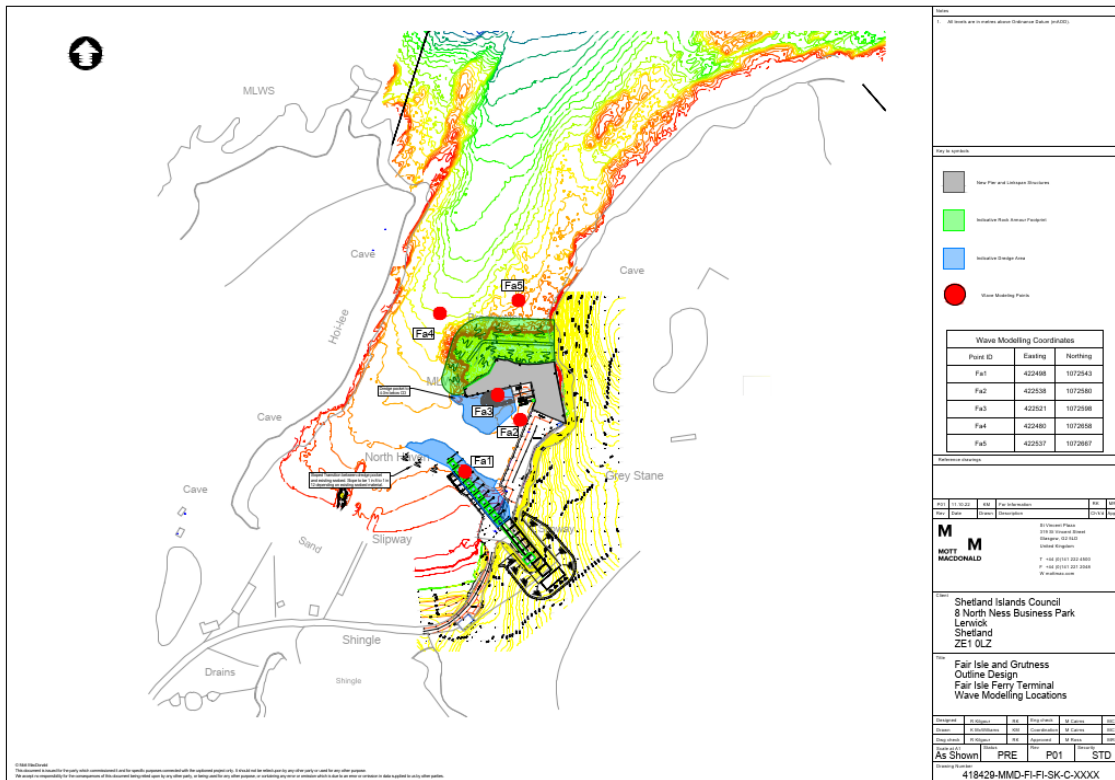


Source: Source: Mott MacDonald, 2023. Contains Delft data, 2022

2.6 Proposed layout

The local wave model incorporated a proposed layout for upgrading the ferry terminal at Fair Isle (Layout 01). This layout and five wave data extraction points used to assess wave conditions at the project site are shown in Figure 2.6.

Figure 2.6: Outline design for the proposed ‘Layout 01’ ferry terminal at Fair Isle.



Source: Mott MacDonald, 2022

2.7 Methodology

The wave modelling approach uses the state-of-the-art numerical wave modelling software, MIKE 21 Flexible Mesh (FM) Spectral Wave (SW) model by DHI⁷. MIKE21 FMSW is a third-generation spectral wind-wave model based on the finite volume method on unstructured meshes that enables full-time domain simulations. The model simulates the growth, decay and transformation of wind-generated waves and swells from offshore to coastal areas and includes wave growth by the action of wind, nonlinear wave-wave interaction, dissipation due to white-capping, dissipation due to bottom friction, dissipation due to depth-induced wave breaking, refraction and shoaling due to depth variations, and the effect of time-varying water depth.

The modelling and analysis methods employed used the best available data to deliver the study objectives. Stages in data acquisition, analysis and model build included:

- Acquisition of bathymetric, topographic and measured and hindcast metocean data from free open access and commercial data sources and the conversion of data to model input formats; and
- European Centre for Medium-Range Weather Forecast (ECMWF) ERA5⁸ hindcast spatial wave and wind data for January 1979 to December 2020 (42 years).

The regional model (Section 3) was built to transform known wave conditions from the offshore ERA-5 extracted location (Figure 2.1) to the boundary of a finer-resolution, local-scale MIKE21

⁷ <https://www.mikepoweredbydhi.com/products/mike-21/waves/spectral-waves>

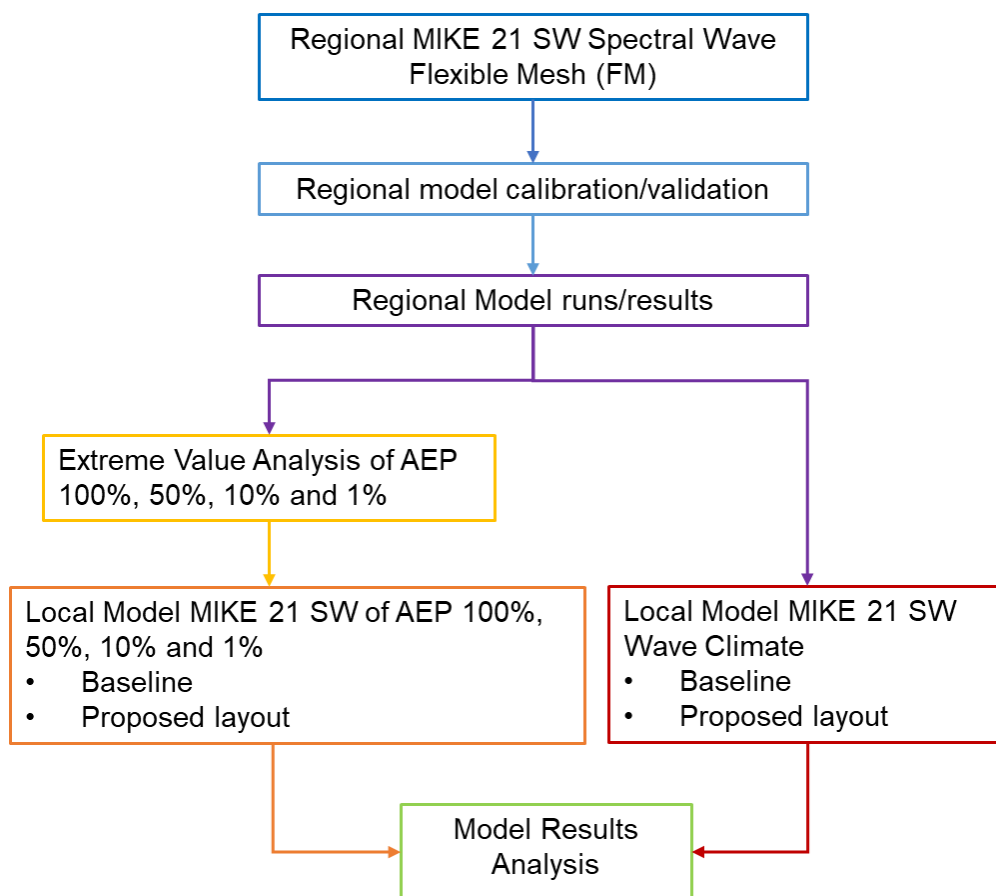
⁸ H. Hersbach et al., “Global reanalysis: goodbye ERA-Interim, hello ERA5,” ECMWF Newsl., no. 159, pp. 17-24, 2019. (<https://cds.climate.copernicus.eu/cdsapp#!/dataset/reanalysis-era5-single-levels?tab=overview>)

FMSW model of Fair Isle (Section 5). In the absence of offshore measured wave data, the regional model was calibrated and validated against historical nearshore wave data at Lerwick (-1.12°E, 60.203°N, Figure 2.1) from 3 April to 7 November 1985. The regional model was run for 42 years, and the outputs were supplied at the local model boundaries.

An extreme value analysis (EVA) (Section 4) was performed at the offshore boundary of the local wave model to estimate the characteristics of waves with 100%, 50%, 10% and 1% Annual Exceedance Probability (AEP). The EVA results were then used in local wave model runs for the existing and proposed layouts.

The local wave model was also run for a representative year to define the annual local wave climate. The year 2018 was selected from the 42-year regional model results as it contained the highest Hs value and is therefore conservative. An overview of the methodology used in this project is shown in Figure 2.7.

Figure 2.7: Methodology followed in the present study.



Source: Mott MacDonald, 2023

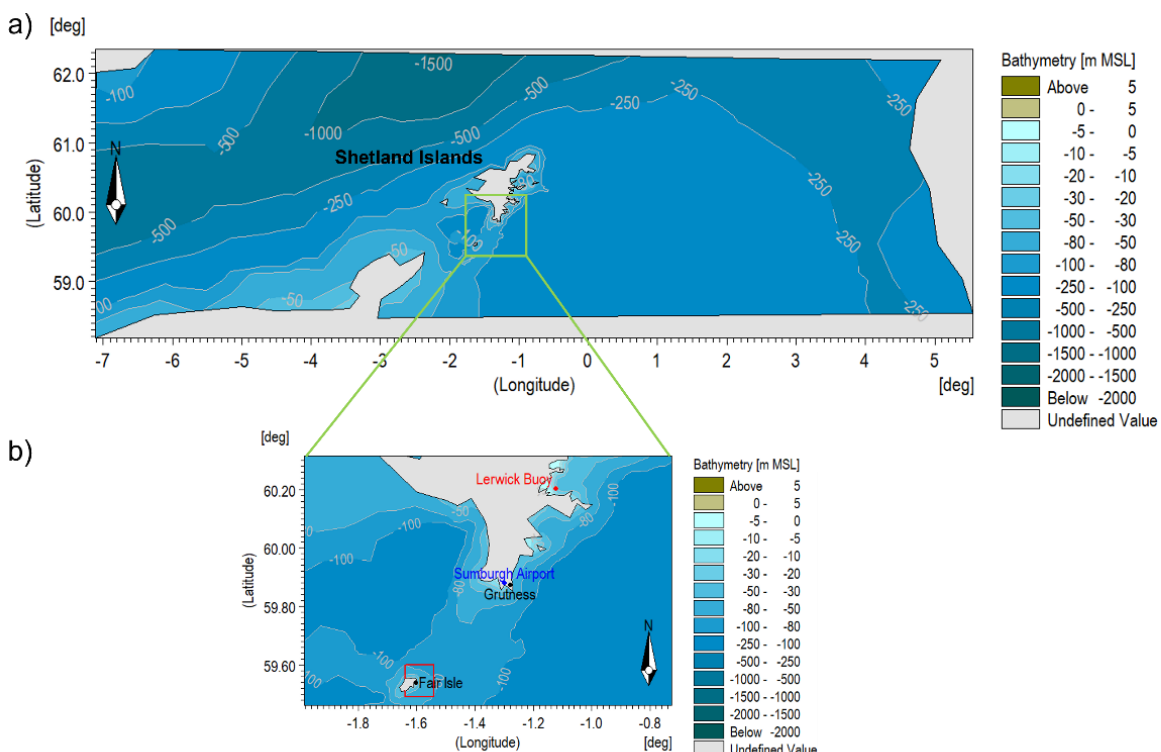
3 Regional MIKE21 FM SW model

The regional MIKE21 FM SW wave model was built to cover a wide area of Shetland Islands and all relevant coastal and offshore areas influencing the wave conditions. It has been used to transform swell waves and local wind-generates waves that propagate into Fair Isle and thereby provide the wave boundary conditions for the local MIKE21 FM SW wave model.

The regional model was entirely built on freely available data from UKHO and EMODnet, prioritising the UKHO data due to better spatial and temporal resolution. **Figure 3.1** shows the MIKE21 FMSW regional model domain and bathymetry. The locations of the Lerwick wave buoy and local wind station at Sumburgh airport are also shown (**Figure 3.1b**).

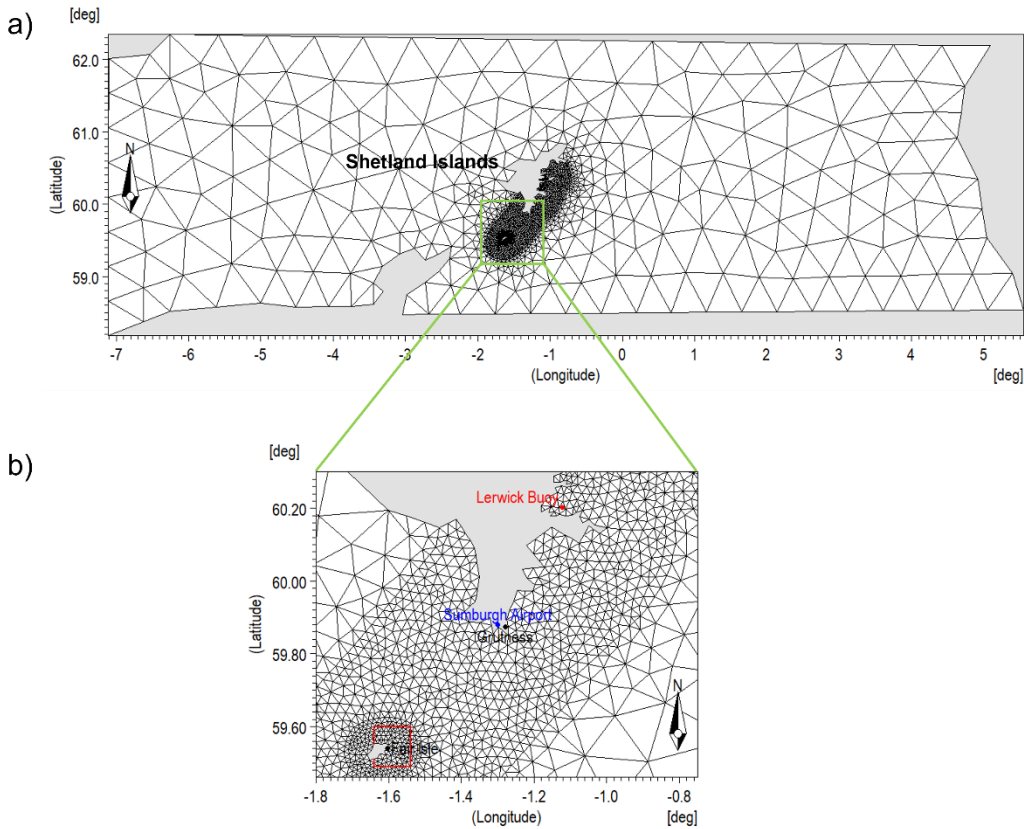
The flexible mesh of the model is shown in **Figure 3.2**. The resolution of the model mesh is coarser in the offshore region (5km to 20km) and finer in the nearshore area around the local model boundary, where the side elements of the mesh are approximately 1500m long.

Figure 3.1: MIKE21 FM SW regional model domain and bathymetry of: (a) the whole regional model; and (b) enlarged view at the Fair Isle model domain boundaries indicated as the red lines.



Source: Mott MacDonald, 2023

Figure 3.2: MIKE21 FM SW regional model domain mesh of: (a) the whole regional model; and (b) enlarged view at the Fair Isle model domain boundaries indicated as the red lines.



Source: Mott MacDonald, 2023

3.1 Model forcing by wind and water levels

The main wind forcing applied as surface boundary conditions was taken from the 42-year ECMWF ERA5 hindcast data set (Section 2.4). Water level conditions were included as time series from the predicted water level at Sumburgh station (Section 2.5) in MSL vertical datum.

3.2 Model Boundary

The boundary conditions for the regional MIKE21 FMSW wave model were extracted from the 42-year ECMWF ERA5 hindcast data set (Section 2.3.2).

3.3 Regional model set up

Several iterative sensitivity tests were undertaken as part of the standard modelling procedures in which different wave parameters were tested to achieve the best model set up (Table 3.1). The wave simulations were run from 1979 to 2020 (42 years).

Table 3.1: Summary of MIKE21 FMSW regional model setup

Parameters	Description	Regional Model
Equation		Fully Spectral, Instationary
Frequency	No. of frequency	25
	Min Frequency	0.04Hz
	Frequency factor	1.1
	Discretisation	
Discretisation	No. of direction	360 degree rose (36 directions)
	Type of threshold	No wind sea and swell separation
	Max threshold (Dynamic)	-
Solution	Threshold frequency	-
		Instationary formulation
	Geographical space discretisation	Low order, fast algorithm
Technique	Max. no of levels in transport calculation	32
	No of steps in source calculation	1
	Min time step	0.01 sec
	Max time step	3600 sec
Water Level Conditions		Varying in time, constant in domain. Measured and predicted levels at Sumburgh (MSL)
Current Conditions		No current included
Wind Forcing	Wind data	Varying in time and domain used downscaled wind data ECMWF ERA-5 (downscaled by 10%. Wind velocities at 10m elevation)
	Soft start	0
	Type of air-sea	Coupled
Ice Coverage	Background Charnock parameter	0.01
		No ice coverage
Diffraction		No diffraction
Energy Transfer		Include quadruplet-wave interaction
Wave Breaking	Model	Wave breaking
	Type of gamma	Specified gamma
	Gamma data	Constant: 0.5
Bottom Friction	Alpha	Constant :1
	Model	No bottom friction
White Capping	Nikuradse roughness data	-
	Current friction	0
	Model	White Capping Included
White Capping	Dissipation Coefficient, C _{dis}	Constant: 4.5
	Dissipation Coefficient, DELTA _{dis}	Constant: 0.5
Structures		No structures
Initial Conditions		Spectra from empirical formula from JONSWAP fetch growth expression
Boundary Conditions		Wind-sea and swell parameters. Varying in time and along line from ECMWF ERA5 (1979-2020)

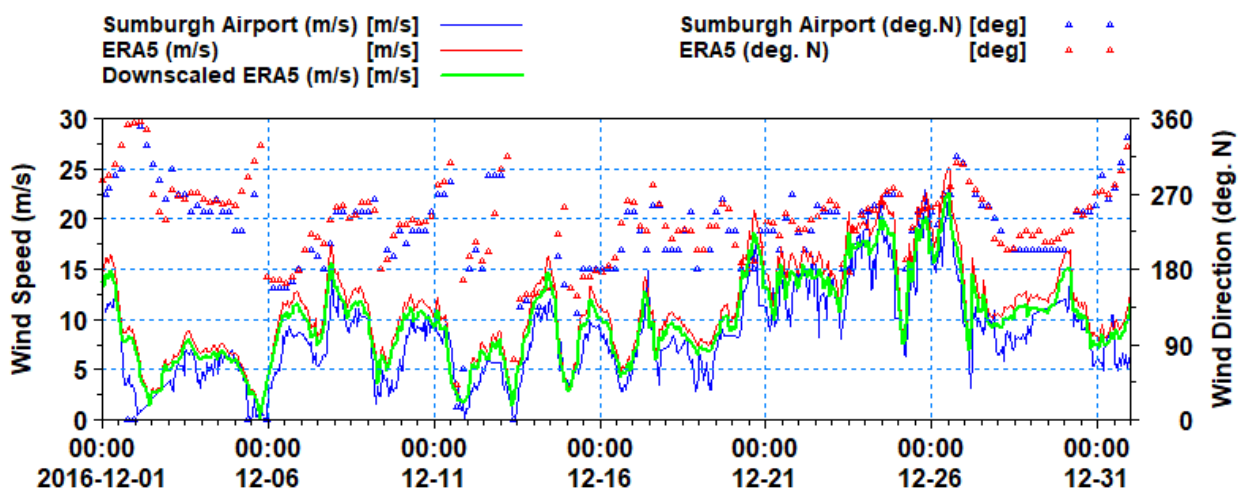
Source: Mott MacDonald, 2023

3.4 Regional model calibration

Wind data from the ECMWF ERA5 dataset was compared with measured wind data from Sumburgh airport (**Figure 3.1 b**), the closest wind station to the Lerwick wave buoy location. This work was undertaken as part of the model calibration to identify ECMWF ERA5 wind speed trends that differed from the locally measured wind data.

Figure 3.3 shows a comparison plot between ERA-5 and measured wind speed at Sumburgh Airport. The figure shows that ECMWF ERA5 wind speed is overestimated compared to the measured wind data at Sumburgh airport. Therefore, following standard modelling practice, the ERA-5 wind speed was downscaled by 10% to improve the agreement between predicted and measured wind speed. The downscaled ERA-5 wind shown in **Figure 3.3** demonstrates better agreement with the measured wind at Sumburgh airport. It is noted that several sensitivity tests were conducted for the model calibration. The selected downscaled ECMWF ERA5 wind speed is generally higher but is considered to be the most conservative.

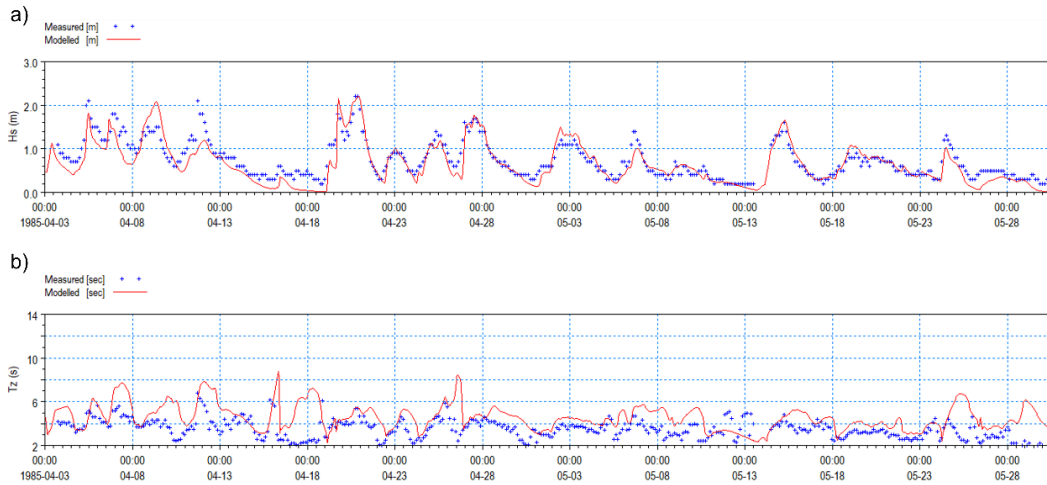
Figure 3.3: Comparison of measured and hindcast wind speed and direction at Sumburgh Airport (Figure 3.1b).



Source: Mott MacDonald, 2023

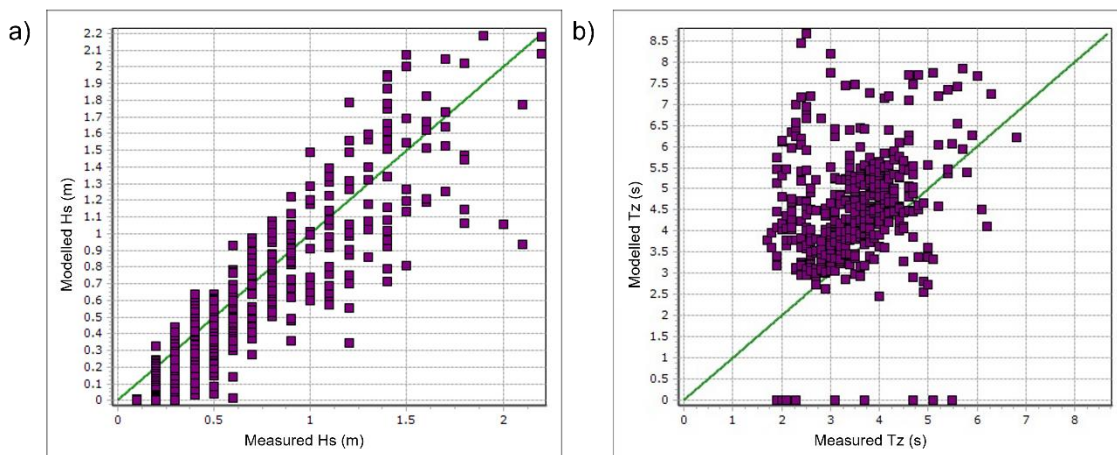
By applying the downscaled ECMWF ERA5 wind data to the regional model for the calibration period between 3 March to 31 May 1985, predicted H_s and T_z values compared well with the wave measurements at Lerwick (**Figure 3.4**). It should be noted that mean wave direction was not available locally and therefore has not been compared. The scatter plot between measured and modelled H_s (**Figure 3.5**) conforms to standard model performance metrics. While the model overestimates T_z , the values are generally two to four seconds and are considered acceptable for the present study.

Figure 3.4: Time series plots showing historical measured waves (blue cross) at Lerwick and regional modelled (red line) data for (a) significant wave height, H_s ; and (b) zero-crossing wave period, T_z for the calibration period (3 March to 31 May 1985).



Source: Mott MacDonald, 2023

Figure 3.5: Scatter plot comparison between: (a) measured wave height, H_s ; and (b) zero-crossing wave period, T_z , at Lerwick against modelled regional results.



Source: Mott MacDonald, 2023

Model performance statistics are shown in Table 3.2 and Table 3.3. These data show that the regional model can replicate measured data with high accuracy for H_s (bias = -0.08m, RMSE = 0.18m and IA = 0.93) and show that the regional model performance meets a satisfactory model standard defined in Williams & Esteves (2017)⁹.

⁹ Williams, J.J. and Esteves, L.S., 2017. Guidance on Setup, Calibration, and Validation of Hydrodynamic, Wave and Sediment Models for Shelf Seas and Estuaries. Advances in Civil Engineering, 5251902, 2017

Table 3.2: Statistics of the comparison between measured wave height and zero-crossing wave period against modelled wave height.

Item Name	Measured Hs (m)	Modelled Hs (m)	Difference Hs (m)	Measured Tz (s)	Modelled Tz (s)	Difference Tz (s)
Minimum	0.10	0.00	0.10	1.7	0.0	1.7
Maximum	2.20	2.18	0.02	6.8	8.7	1.9
Average	0.73	0.66	0.07	3.5	4.5	1.0
Std. deviation	0.43	0.47	0.04	0.9	1.3	0.4

Source: Mott MacDonald, 2023

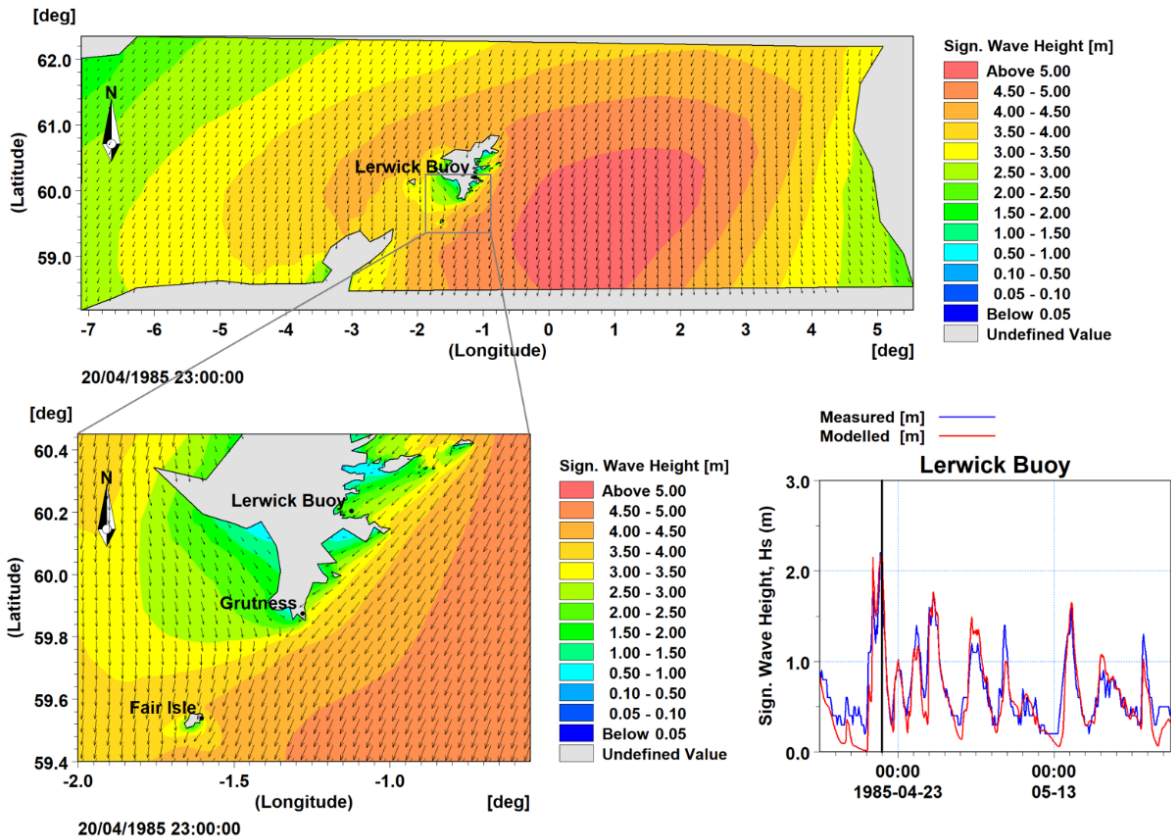
Table 3.3: Performance measured of the comparison between measured wave height and zero-crossing wave period at Lerwick against modelled wave height and zero-crossing wave period.

Statistic	Hs Value	Tz Value
Mean Error	0.10 (m)	1.0 (s)
Mean Absolute Error	0.18 (m)	1.3 (s)
Root Mean Square Error	0.23 (m)	1.7 (s)
Std. dev of Residuals	0.22 (m)	1.4 (s)
Coefficient of Determination	0.78 (no unit)	0.06 (no unit)
Coefficient of Efficiency	0.74 (no unit)	-0.71 (no unit)
Index of Agreement	0.93 (no unit)	0.48(no unit)

Source: Mott MacDonald, 2023

Figure 3.6 shows regional wave model results during a storm on 20 April 1985 at 23:00 UTC. The storm was recorded by the Lerwick buoy and confirmed that the dominant wave direction was from the northeast. **Figure 3.6** demonstrates that the model predictions generally compare well with the measured data.

Figure 3.6: Significant wave height (Hs) predicted by the regional MIKE21 FM SW model during the storm's peak on 20 April 1985 at 23:00 UTC.

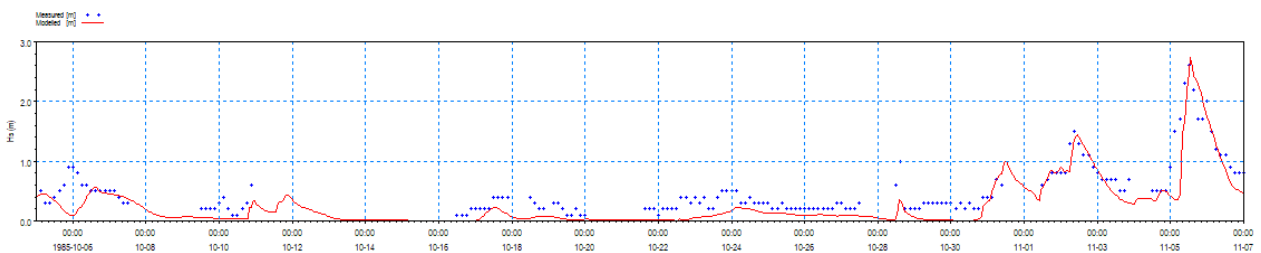


Source: Mott MacDonald, 2023

3.5 Regional model validation

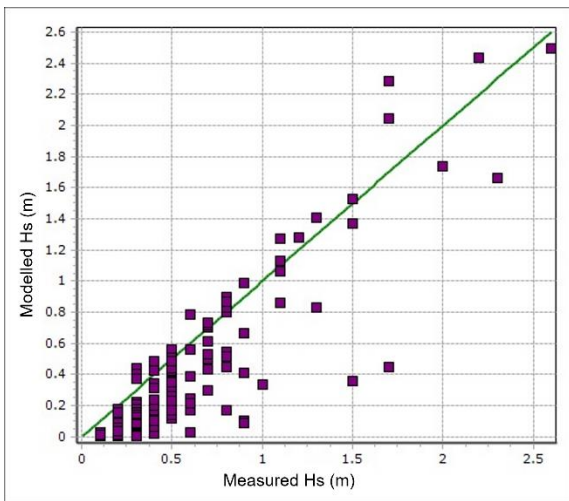
The measured data from the Lerwick wave buoy for 5 October to 7 November 1985 was used to validate the regional model. **Figure 3.7** shows a comparison plot between measured and modelled data at Lerwick buoy location for Hs only (historically measured of Tz and MWD data are unavailable). The modelled Hs in **Figure 3.8** shows that the model replicates well the observed wave conditions for the validation period.

Figure 3.7: Time series plots showing historical measured waves (blue cross) at Lerwick and regional modelled (red line) data for the significant wave height, Hs, for the validation period (5 October to 7 November 1985).



Source: Mott MacDonald, 2023

Figure 3.8: Scatter plot comparison between measured wave height and at Lerwick against modelled regional results.



Source: Mott MacDonald, 2023

Statistics to quantify the model performance are summarised in Table 3.4 and Table 3.5. It is considered that the regional model again reproduces wave conditions in this study accurately. Therefore, the calibrated and validated regional model is judged to be suitable to provide boundary conditions for the local models.

Table 3.4: Statistics of the comparison between measured wave height

Item Name	Measured Hs (m)	Modelled Hs (m)	Difference Hs (m)
Minimum	0.10	0.00	0.10
Maximum	2.60	2.50	0.10
Average	0.50	0.33	0.17
Std. deviation	0.44	0.47	0.02

Source: Mott MacDonald, 2023

Table 3.5: Performance measured of the comparison between measured wave height at Lerwick against modelled wave height for the validation period.

Statistic	Hs Value
Mean Error	0.17 (m)
Mean Absolute Error	0.20 (m)
Root Mean Square Error	0.27 (m)
Std. dev of Residuals	0.21 (m)
Coefficient of Determination	0.80 (no unit)
Coefficient of Efficiency	0.67 (no unit)
Index of Agreement	0.91 (no unit)

Source: Mott MacDonald, 2023

4 Extreme value analysis

An extreme value analysis (EVA) was performed using the DHI EVA Toolbox¹⁰ on the regional wave model results to define wave characteristics associated with 100%, 50%, 10% and 1% AEP events. These conditions were subsequently applied at the local wave model boundaries.

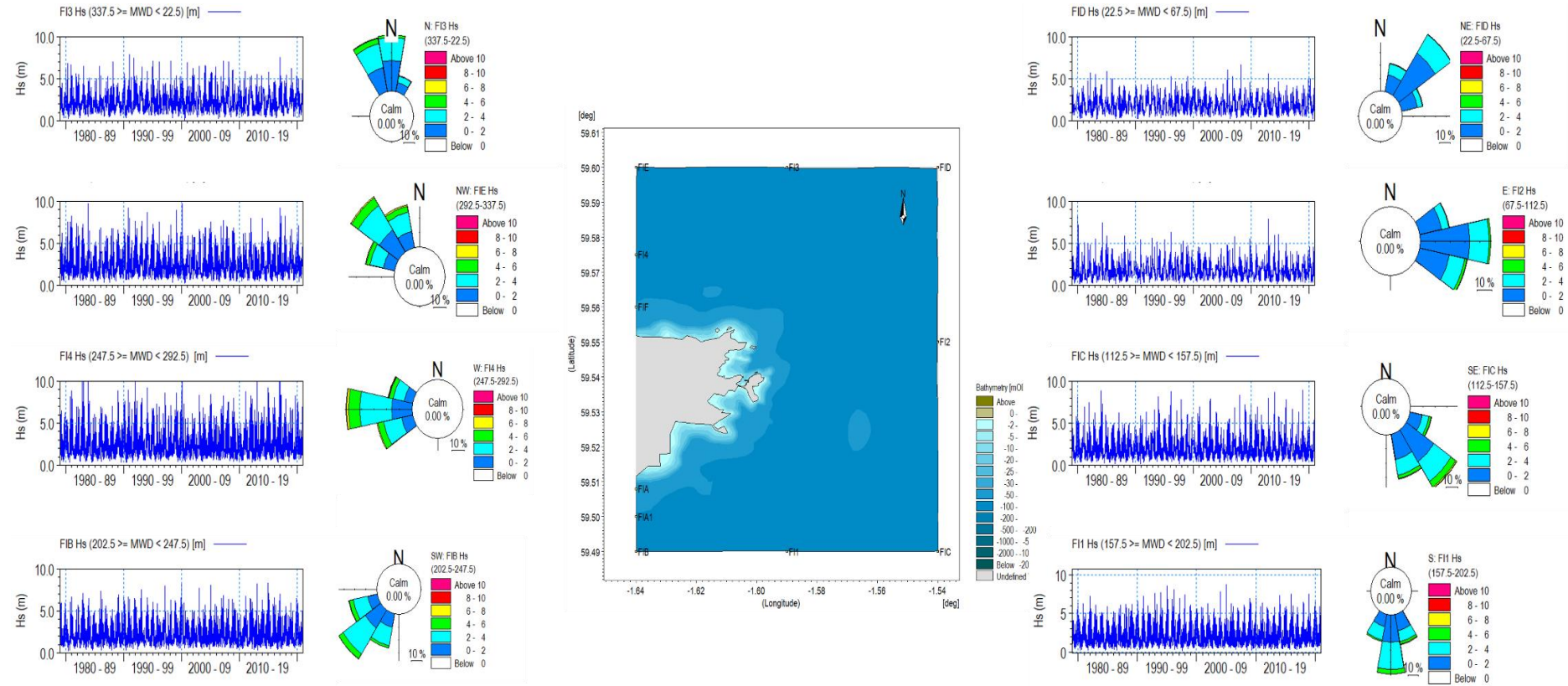
4.1 EVA of Hs

The EVA of Hs was conducted using data extracted from the regional wave model at the local wave boundaries locations FI4, FIE, FI3, FID, FI2, FIC, FI1 and FIB (Figure 4.1). Hs values at each boundary point were also analysed based on eight directional wave sectors as follows:

- West (W): FI4 $247.5 \geq \text{MWD} < 292.5$ deg.N
- North West (NW): FIE $292.5 \geq \text{MWD} < 337.5$ deg.N
- North (N): FI3 $337.5 \geq \text{MWD} < 22.5$ deg.N
- North East (NE): FID $22.5 \geq \text{MWD} < 67.5$ deg. N
- East (E): FI2 $67.5 \geq \text{MWD} < 112.5$ deg.N
- South East (SE): FIC $112.5 \geq \text{MWD} < 157.5$ deg.N
- South (S): FI1 $157.5 \geq \text{MWD} < 202.5$ deg. N
- South West (SW): FIB $202.5 > \text{MWD} < 247.5$ deg.N

¹⁰ https://manuals.mikepoweredbydhi.help/latest/General/EVA_SciDoc.pdf accessed on 13 September 2022.

Figure 4.1: Location of waves data extraction at FI 4, FIE, FI3, FID, FI2, FIC, FI1 and FIB with the filtered Hs rose plot based on the selected dominant directional sector.



Source: Mott MacDonald, 2023

The best-fit probability distribution curves to the extreme Hs data for each selected wave sector are shown in Figure 4.2, with lines showing the 95% confidence intervals.

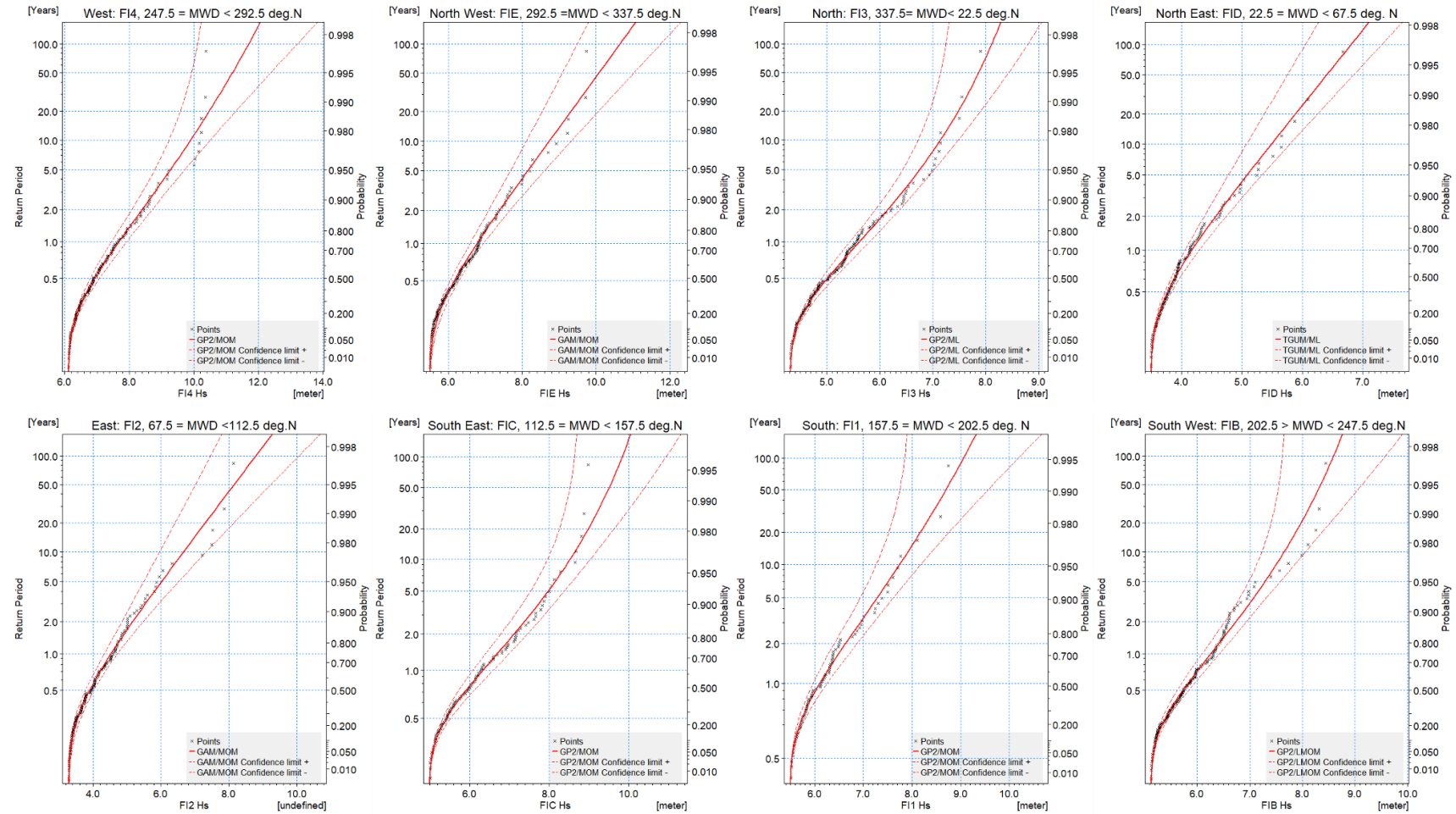
4.1 Tp and Hs relationship

Due to various environmental factors, wave periods were highly variable, and thus, wave periods associated with given wave heights were obtained using the relationship between predicted Tp and Hs values (Figure 4.3). The resulting Tp values applied as boundary conditions for each AEP in the local wave model simulations are shown in Table 4.1

4.2 Wind Speed and Hs relationship

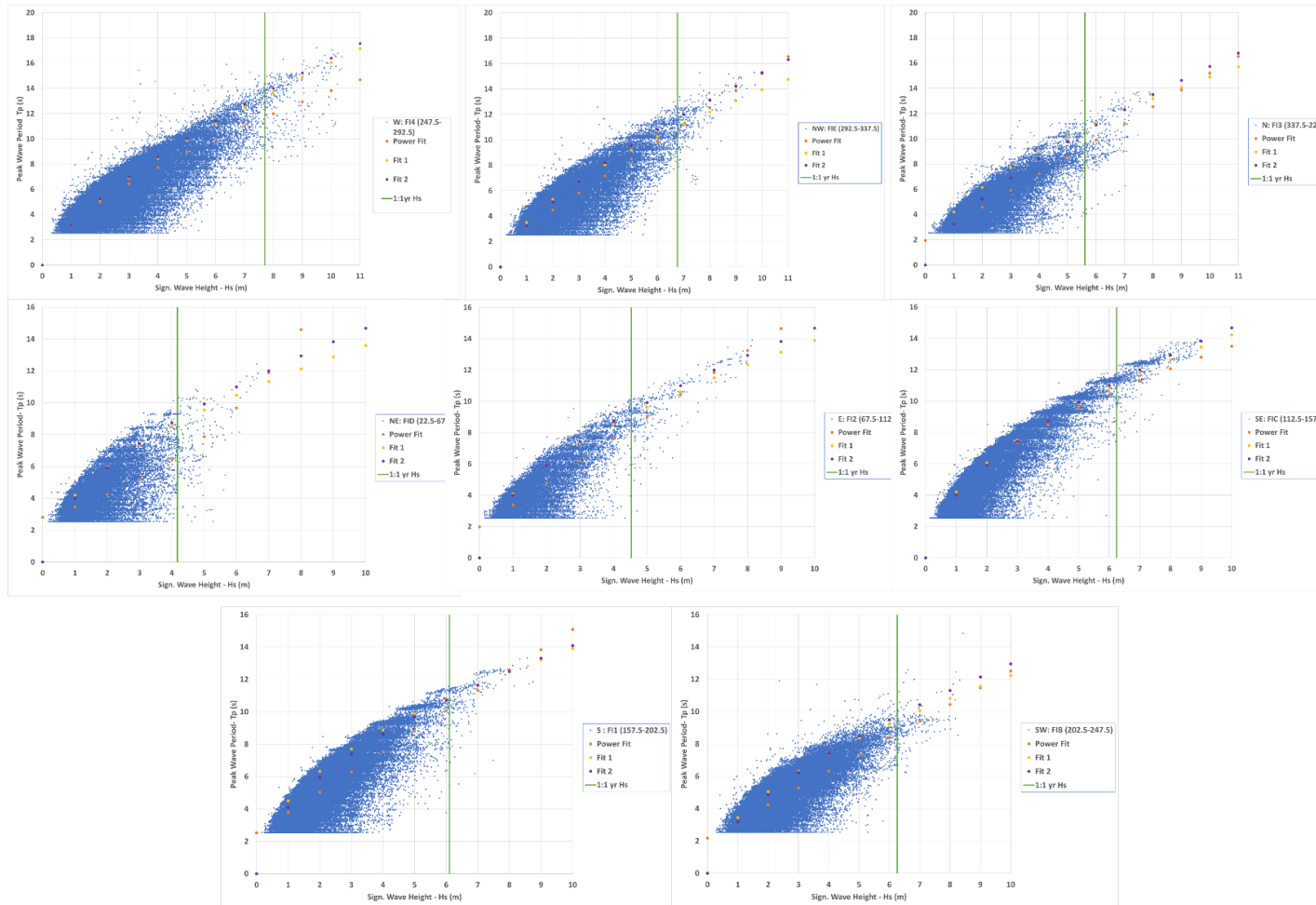
The relationship between wind and wave height was obtained for the eight directional sectors (Figure 4.4). The resulting extreme wind speeds are tabulated in Table 4.1.

Figure 4.2: Probability distribution fit of Hs at the eight dominant directional sectors (N, NE, E, SE, E, SW, W, NW)



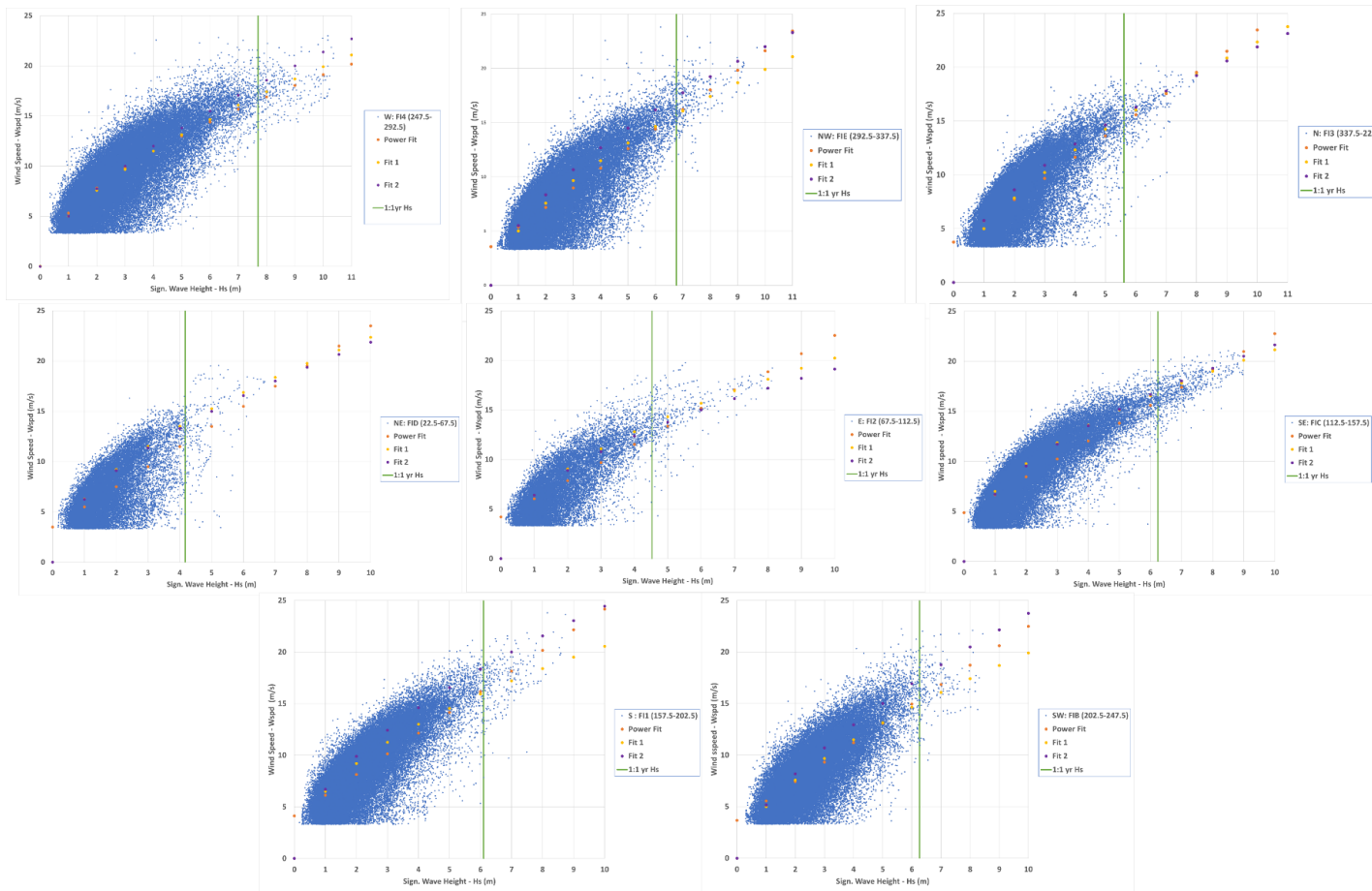
Source: Mott MacDonald, 2023

Figure 4.3: Relationship between T_p and H_s at the directional sectors (N, NE, E, SE, E, SW, W, NW) with the 100% AEP (1:1 year RP) of H_s .



Source: Mott MacDonald, 2023

Figure 4.4: Relationship between wind speed and Hs at the directional sectors (N, NE, E, SE, E, SW, W, NW).



Source: Mott MacDonald, 2023

4.3 Extreme wave conditions

Table 4.1 summarises extreme Hs, Tp and wind speed obtained from the EVA for the 100%, 50%, 10% and 1% AEP. The water level condition at HAT from the Fair Isle station was selected as the extreme water level in the wave model runs for each AEP event to be conservative. The MWD and wind direction used the same eight directional sectors (N, NE, E, SE, E, SW, W, NW) at 11.25-degree intervals.

Table 4.1: Summary of the wave and wind conditions for the local wave model simulations for each AEP event.

	AEP (%)	100	50	10	1
Sector	Return period (year)	1	2	10	100
W (247.5>=MWD<292.5)	Hs (m)	7.70	8.40	9.90	11.70
	Tp (s)	13.6	14.5	16.2	18.3
	Wspd (m/s)	18.1	19.1	21.2	23.6
NW (292.5>=MWD<337.5)	Hs (m)	6.77	7.36	8.74	10.65
	Tp (s)	11.7	12.4	13.9	16.0
	Wspd (m/s)	17.4	18.3	20.3	22.8
N (337.5>=MWD<22.5)	Hs (m)	5.61	6.15	7.11	8.11
	Tp (s)	10.6	11.3	12.5	13.6
	Wspd (m/s)	15.6	16.5	18.0	19.4
NE (22.5>=MWD<67.5)	Hs (m)	4.17	4.60	5.46	6.81
	Tp (s)	9.0	9.5	10.4	11.8
	Wspd (m/s)	13.8	14.6	16.0	18.1
E (67.5>=MWD<112.5)	Hs (m)	4.53	5.17	6.61	8.79
	Tp (s)	9.4	10.1	11.6	13.6
	Wspd (m/s)	13.6	14.6	16.5	19.0
SE (112.5>=MWD<157.5)	Hs (m)	6.35	7.12	8.48	9.83
	Tp (s)	11.4	12.1	13.4	14.5
	Wspd (m/s)	17.2	18.2	19.9	21.4
S (157.5>=MWD<202.5)	Hs (m)	6.10	6.64	7.71	9.06
	Tp (s)	10.8	11.3	12.3	13.4
	Wspd (m/s)	18.5	19.4	21.1	23.1
SW (202.5>=MWD<247.5)	Hs (m)	6.26	6.73	7.62	8.59
	Tp (s)	9.7	10.2	11.0	11.8
	Wspd (m/s)	17.4	18.3	19.8	21.5

Source: Mott MacDonald, 2023

5 Local MIKE21 FMSW model

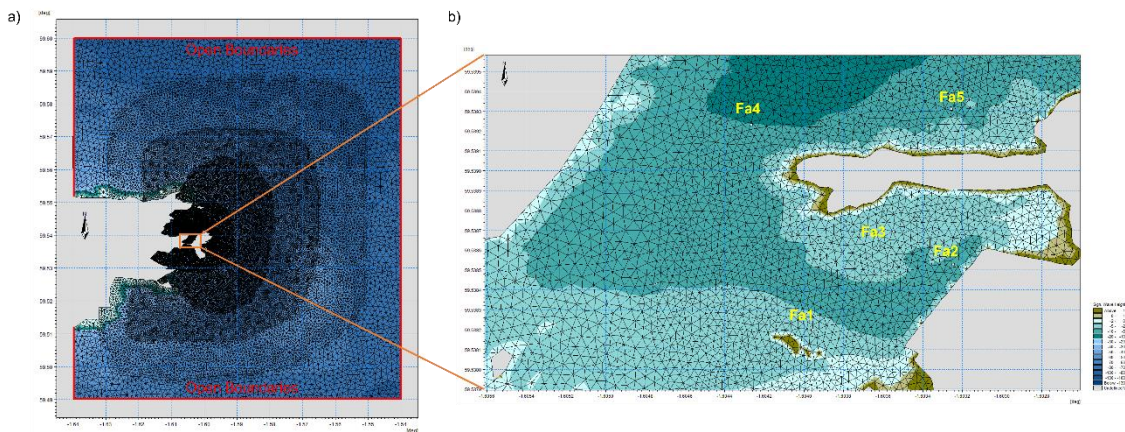
A local MIKE21 FMSW model of Fair Isle was built and used to transform offshore waves to the project site. Calibration of the local model was not undertaken as no suitable wave measurements were available.

5.1 Fair Isle local model domain

The local wave model domain was designed to be sufficiently large to ensure an accurate representation of wave propagation to the study area. Figure 5.1 shows the model’s flexible mesh, open boundary locations and model bathymetry. The horizontal and vertical datums of the model were set as geographical coordinate (longitude/latitude) and ordnance datum Newlyn (ODN), respectively. Similar to the regional model, the processed bathymetry data in Section 2.2 was linearly interpolated across the local model flexible mesh using the Mesh Generator toolbox.

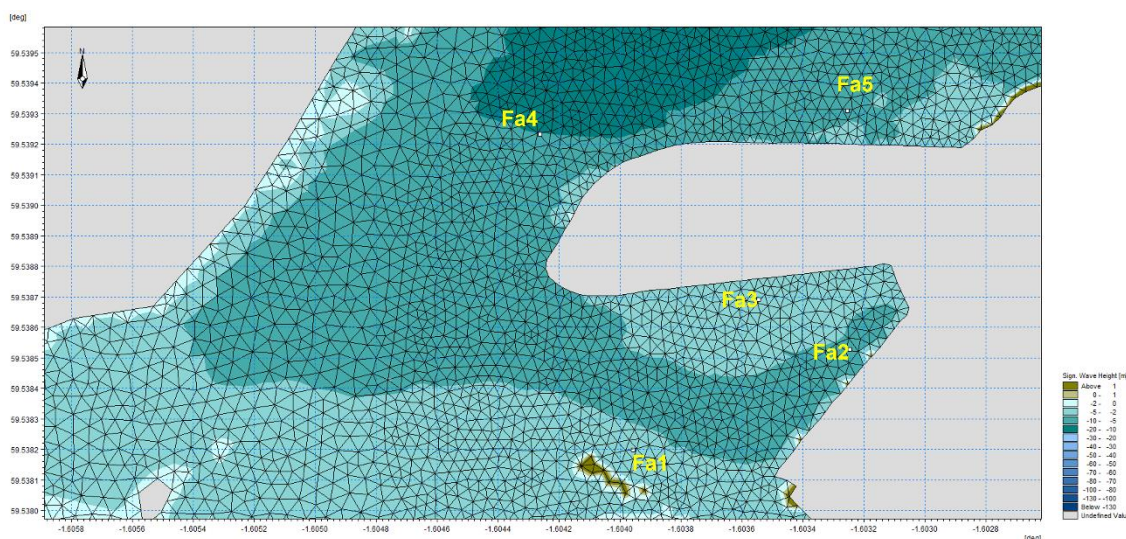
The model domain shown in Figure 5.1 defines the baseline layout. The resolution of the outer model domain varies between approximately 20m and 400m. In the nearshore areas within the baseline layout, the mesh resolution varies between approximately 5m and 10m. The proposed ferry terminal was incorporated into the local model by keeping the same local model domain extent and resolution. An enlarged view of the local model mesh and bathymetry of the proposed layout is shown in Figure 5.2. The five wave data extraction points (Fa1, Fa2, Fa3, Fa4 and Fa5) are also shown in all local model domains (Figure 5.1b and Figure 5.2).

Figure 5.1: Local model bathymetry and mesh of: (a) the whole local model domain with open boundary locations indicated as the red lines; and (b) an enlarged view of the existing breakwater at the project site.



Source: Mott MacDonald, 2023

Figure 5.2: Enlarged view of mesh and bathymetry of the proposed ‘Layout 01’ with data extraction location points (Fa1, Fa2, Fa3, Fa4 and Fa5) to assess wave conditions.



Source: Mott MacDonald, 2023

5.2 Fair Isle model set up

Several iterative sensitivity tests were undertaken as part of the standard modelling procedures and different wave parameters were tested to achieve the best model set up (Table 5.1).

Table 5.1: Summary of MIKE21 FMSW local model set up

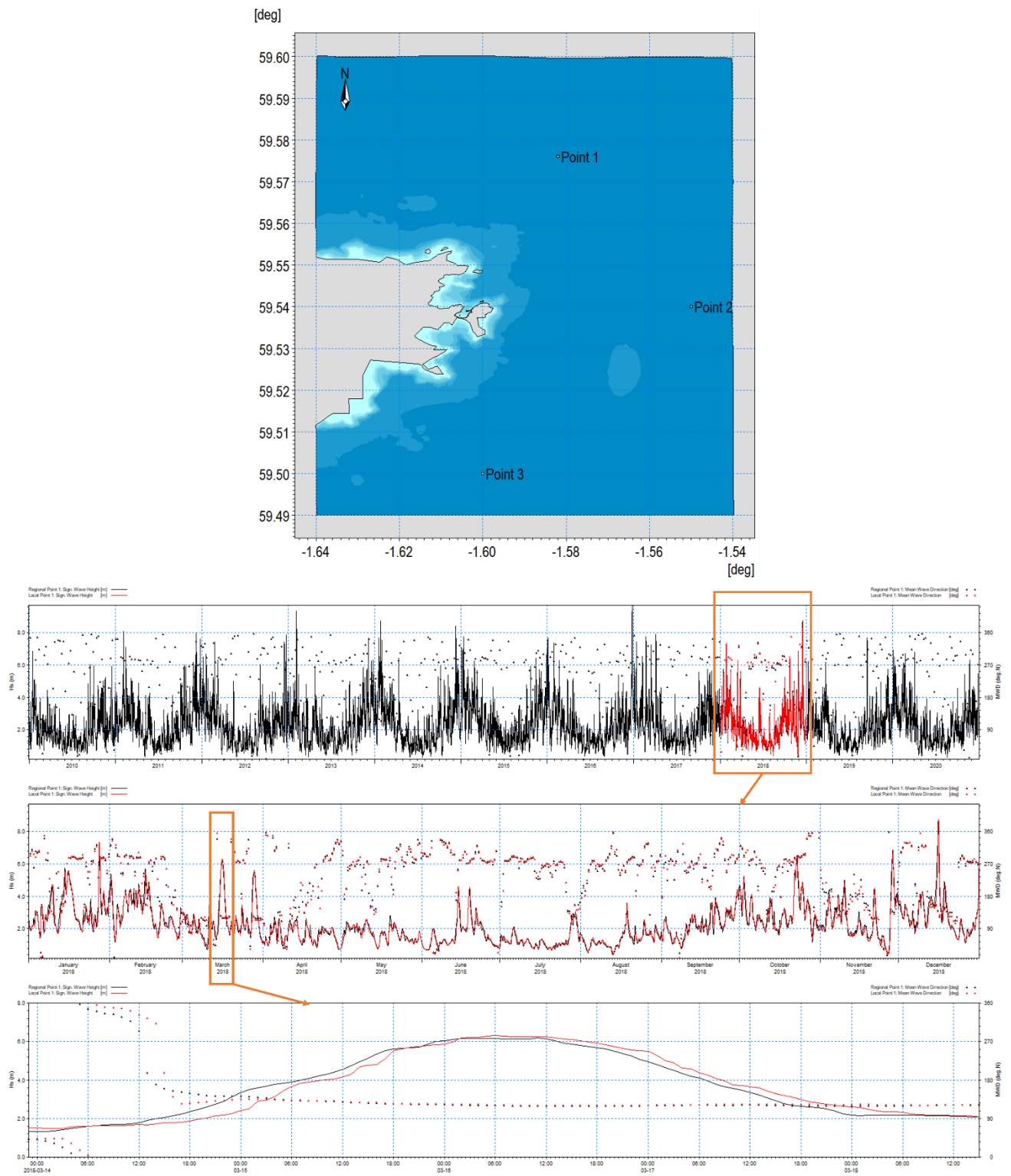
Parameters	Description Local Model	
Equation	Directional-Decoupled, Quasi-stationary	
Quasi-stationary formulation	Geographical space discretisation	Low-order, fast algorithm
	Method	New-Raphson Iteration
	Max. number of iterations	100
	Tolerance (RMS-norm of residual)	0.01
	Tolerance (Max-norm of change in sig. wave height)	0.05
	Relaxation Factor	0.1
Water Level Conditions	<ul style="list-style-type: none"> Varying in time, constant in domain. Measured and predicted levels at Sumburgh in ODN for the wave climate simulation. HAT for the AEP simulations. 	
Current Conditions	No current included	
Wind Forcing	Wind data	<ul style="list-style-type: none"> Varying in time and domain used downscaled wind data ECMWF ERA-5 (downscaled by 10%. Wind velocities at 10m elevation) for the wave climate simulation. Wind speed and direction from the EVA results for the AEP simulations
	Wind Generation Formula	SPM84
Diffraction	No diffraction	
Wave Breaking	Model	Wave breaking

Parameters		Description Local Model
	Type of gamma	Specified gamma
	Gamma data	0.8
	Alpha	1
	Gamma (wave steepness)	5
Structures	Line Structure	West Cliff face Type of transmission: Constant transmission Coefficient: 0 Reflection: Full reflection
Initial Conditions		Spectra from empirical formula from JONSWAP fetch growth expression
Boundary Conditions		<ul style="list-style-type: none"> Wave parameters extracted from the calibrated regional model results for wave climate simulation. Wave parameters from the EVA results for the AEP simulations.

Source: Mott MacDonald, 2023

Although calibration of the local wave model was not performed due to the absence of measured local data, a comparison between the regional and local models was undertaken at an offshore location (Point 1), shown in Figure 5.3. This figure compares wave height and mean wave direction time series at a range of temporal resolutions. The agreement is good, indicating that offshore to nearshore wave transformation by the local wave model is accurate. Additional comparisons for the other offshore locations, 'Point 2' and 'Point 3', are presented in Appendix A and show equally good agreement.

Figure 5.3: Location of Point 1 and Hs time series from the regional and local wave models.



Source: Mott MacDonald, 2023

6 Results

6.1 AEP results

Table 6.1 shows, at extraction points Fa1, Fa2, Fa3, Fa4 and Fa5 (Figure 5.2), the highest predicted Hs and associated Tp and MWD values for each AEP scenario for the baseline and 'Layout 01' conditions. As expected, due to sheltering behind the breakwater, Hs values at Fa1, Fa2 and Fa3 for 'Layout 01' are less than values for the baseline.

Table 6.2 shows the highest predicted Tp values with the associated Hs and MWD values at Fa1, Fa2 and Fa3 for each AEP scenario for the baseline and 'Layout 01'.

Table 6.1: AEP results at extraction points (Fa1, Fa2, Fa3, Fa4 and Fa5) for the existing and 'Layout 01' for the high Hs.

Point	AEP (%)	RP	Baseline			Layout 01		
			Highest Hs (m)	Associated Tp (s)	Associated MWD (deg. N)	Highest Hs (m)	Associated Tp (s)	Associated MWD (deg. N)
Fa1	100	1	0.3	8	344	0.3	6	328
	50	2	0.3	9	344	0.3	8	333
	10	10	0.4	11	344	0.4	10	331
	1	100	0.5	14	342	0.5	13	332
Fa2	100	1	0.2	6	296	0.2	3	229
	50	2	0.2	9	294	0.2	3	229
	10	10	0.2	11	293	0.1	3	232
	1	100	0.3	14	291	0.2	3	232
Fa3	100	1	0.2	9	270	0.2	3	222
	50	2	0.3	10	270	0.2	3	220
	10	10	0.3	11	271	0.2	3	222
	1	100	0.4	14	271	0.2	3	221
Fa4	100	1	1.0	10	14	1.0	10	17
	50	2	1.3	11	14	1.2	11	17
	10	10	1.6	12	15	1.5	12	17
	1	100	2.1	16	16	2.1	16	17
Fa5	100	1	1.3	10	354	1.2	10	355
	50	2	1.5	11	353	1.4	11	354
	10	10	1.9	12	352	1.8	12	353
	1	100	2.7	16	351	2.6	16	351

Source Mott MacDonald, 2023

Table 6.2: AEP results at Fa1, Fa2 and Fa3 (extraction points behind the breakwater) for the baseline and 'Layout 01' for the high Tp.

Point	AEP	RP	Baseline			Layout 01		
			Associated Hs (m)	Longest Tp (s)	Associated MWD (deg. N)	Associated Hs (m)	Longest Tp (s)	Associated MWD (deg. N)
Fa1	100	1	0.3	9	339	0.3	8	331
	50	2	0.3	10	341	0.3	9	332
	10	10	0.2	14	342	0.4	12	330
	1	100	0.3	18	343	0.3	17	332
Fa2	100	1	0.2	9	293	0.1	4	298
	50	2	0.2	10	293	0.1	5	300
	10	10	0.2	13	293	0.1	8	277
	1	100	0.3	15	292	0.1	12	283
Fa3	100	1	0.2	10	267	0.1	4	276
	50	2	0.3	11	266	0.1	5	273
	10	10	0.3	13	269	0.1	7	259
	1	100	0.3	17	270	0.1	12	259

Source Mott MacDonald, 2023

6.2 Wave climate results

Data from the local model run for 2018 were obtained and analysed at the five extraction points (Figure 5.2). The resulting mean statistics of Hs, Tp and MWD for the baseline and 'Layout 01' are shown in Table 6.3. Table 6.4 shows the results of the high Hs with the associated Tp and MWD for the baseline and 'Layout 01' conditions. Table 6.4 shows that Hs decreased at Fa2 and Fa3 for 'Layout 01' as expected due to their locations (i.e. sheltered behind the breakwater).

Table 6.5 shows the results of the highest Tp with the associated Hs and MWD at Fa1, Fa2 and Fa3 (extraction points behind the breakwater) for the baseline and 'Layout 01'. High Tp's are still present at 'Layout 01' at those locations due to reflection and directional spreading (Table 6.5).

Table 6.3: Annual mean wave conditions at the five extraction points for the baseline and 'Layout 01'.

Point	Baseline			Layout 01		
	Mean Hs (m)	Mean Tp (s)	Mean MWD (deg.N)	Mean Hs (m)	Mean Tp (s)	Mean MWD (deg.N)
Fa1	0.1	12	313	0.13	12	328
Fa2	0.1	12	281	0.04	12	280
Fa3	0.1	12	254	0.02	12	249
Fa4	0.4	12	20	0.35	12	14
Fa5	0.4	12	345	0.41	12	345

Source: Mott MacDonald, 2023

Table 6.4: High Hs conditions at the five extraction points for the baseline and 'Layout 01'.

Point	Baseline			Layout 01		
	Highest Hs (m)	Associated Tp (s)	Associated MWD (deg.N)	Highest Hs (m)	Associated Tp (s)	Associated MWD (deg.N)
Fa1	0.5	14	341	0.6	14	329
Fa2	0.3	14	289	0.2	14	283
Fa3	0.4	14	262	0.2	3	225
Fa4	1.6	14	8	1.5	14	12
Fa5	1.7	14	346	1.7	14	346

Source: Mott MacDonald, 2023

Table 6.5: High Tp conditions at Fa1, Fa2 and Fa3 for the baseline and 'Layout 01'.

Point	Baseline			Layout 01		
	Associated Hs (m)	Highest Tp (s)	Associated MWD (deg.N)	Associated Hs (m)	Highest Tp (s)	Associated MWD (deg.N)
Fa1	0.0	22	189	0.27	19	328
Fa2	0.0	20	238	0.08	19	281
Fa3	0.2	19	252	0.05	19	247

Source: Mott MacDonald, 2023

6.3 Annual wave occurrences

Examples of the annual wave occurrences of Hs and Tp for the baseline and 'Layout 01' at Fa3 are shown in Table 6.6 and Table 6.7, respectively. For the proposed 'Layout 01' Hs decreased at Fa3 as it is sheltered behind the breakwater, while high Tp values are observed at the same location due to reflection and directional spreading.

The annual wave occurrences of Hs and Tp at Fa1, Fa2, Fa4 and Fa5 for the baseline and 'Layout 01' conditions are presented in Appendix B.1 and B.2, respectively.

Table 6.6: Annual wave occurrence of Hs (m) against Tp (s) at Fa3 for the baseline.

Hs (m) Tp (s)	0-0.1	0.1-0.2	0.2-0.3	0.3-0.4	0.4-0.5	0.5-0.6	Total	Total (%)
0-2	0	0	0	0	0	0	0	0
2-4	0	2	0	0	0	0	2	0
4-6	1	1	0	0	0	0	2	0
6-8	129	3	0	0	0	0	132	2
8-10	1095	386	8	0	0	0	1489	17
10-12	2503	558	78	0	0	0	3139	36
12-14	1657	605	133	11	0	0	2406	28
14-16	586	393	38	1	0	0	1018	12
16-18	63	260	29	6	0	0	358	4
18-20	0	49	31	0	0	0	80	1
20-22	0	0	0	0	0	0	0	0
22-24	0	0	0	0	0	0	0	0
Total	6034	2257	317	18	0	0	8626	
Total (%)	70.0	26.2	3.7	0.2	0.0	0.0		100

Source: Mott MacDonald, 2023

Table 6.7: Annual wave occurrence of Hs (m) against Tp (s) at Fa3 for 'Layout 01'.

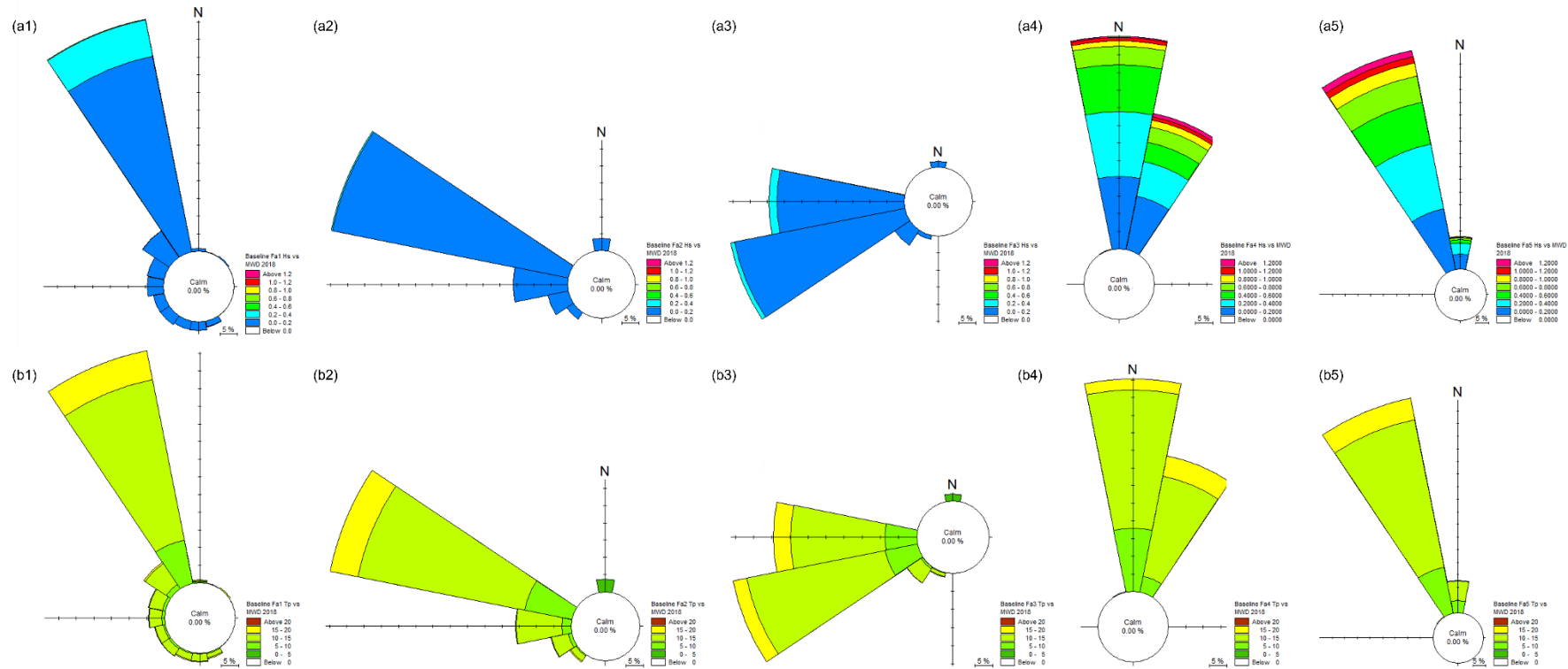
Hs (m) Tp (s)	0-0.1	0.1-0.2	0.2-0.3	0.3-0.4	0.4-0.5	0.5-0.6	Total	Total (%)
0-2	0	0	0	0	0	0	0	0
2-4	11	6	0	0	0	0	17	0
4-6	21	0	0	0	0	0	21	0
6-8	189	0	0	0	0	0	189	3
8-10	1394	0	0	0	0	0	1394	20
10-12	2085	0	0	0	0	0	2085	31
12-14	1772	0	0	0	0	0	1772	26
14-16	901	0	0	0	0	0	901	13
16-18	349	0	0	0	0	0	349	5
18-20	86	0	0	0	0	0	86	1
20-22	0	0	0	0	0	0	0	0
22-24	0	0	0	0	0	0	0	0
Total	6808	6	0	0	0	0	6814	
Total (%)	99.9	0.1	0.0	0.0	0.0	0.0		100

Source: Mott MacDonald, 2023

For the baseline, wave rose plots of H_s and T_p against MWD at Fa1, Fa2, Fa3, Fa4 and Fa5 are shown in Figure 6.1 (a1 to a5) and Figure 6.1 (b1 to b5), respectively. It is observed that the dominant wave direction is from northwest to north at Fa4 and Fa5, while the dominant wave direction for sheltered locations is southwest to the west (Fa2 and Fa3). Fa1 share the same dominant wave direction due to wave reflection.

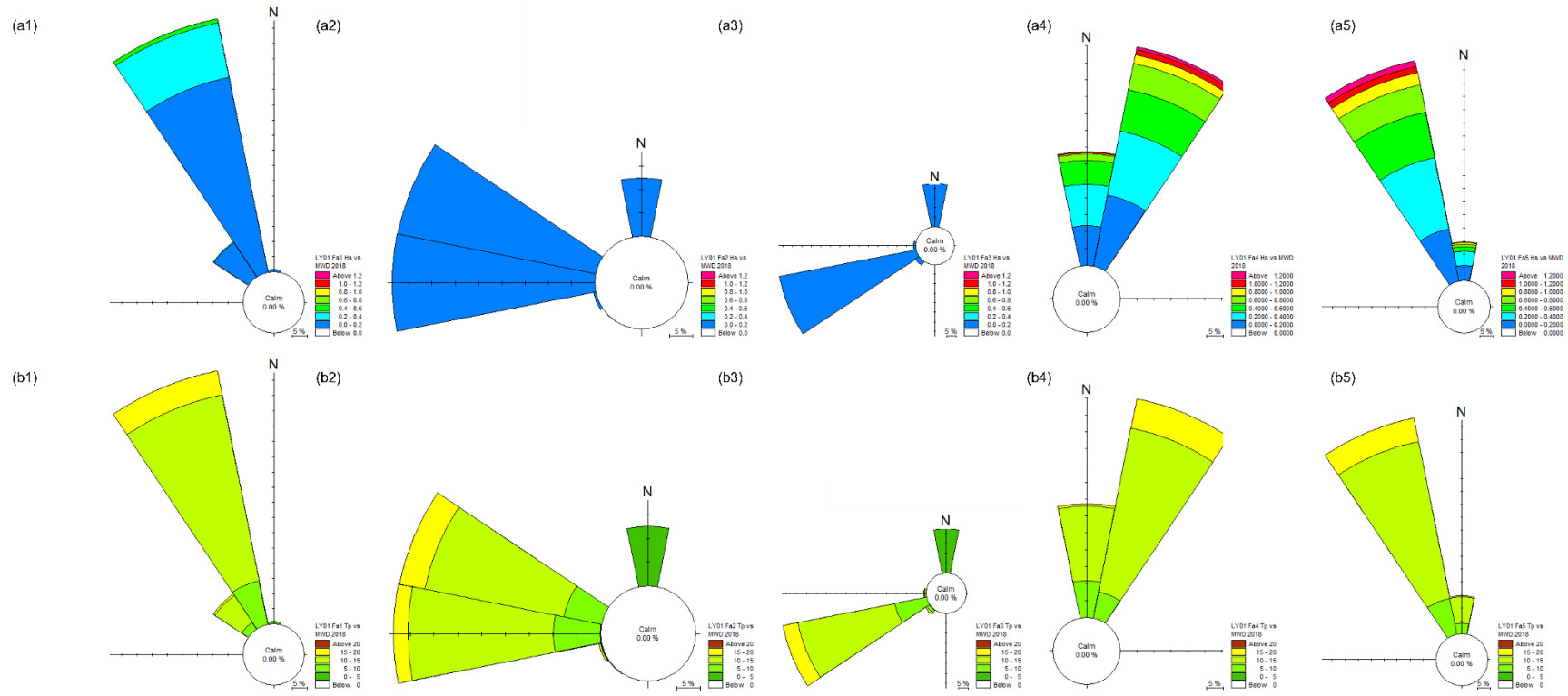
For 'Layout 01' conditions, wave rose plots of H_s and T_p against MWD at Fa1, Fa2, Fa3, Fa4 and Fa5 are shown in Figure 6.2 (a1 to a5) and Figure 6.2 (b1-b5), respectively. The dominant wave direction remains approximately the same as the baseline case with a slight variation at Fa2 and Fa3, where waves coming from the north are marginally more frequent due to the shape of the proposed layout.

Figure 6.1: Wave rose plots at Fa1, Fa2 Fa3, Fa4 and Fa5 for Hs (m) against MWD (deg.N) (a1-a5) and Tp (s) against MWD (deg.N) (b1-b5) for the baseline conditions.



Source: Mott MacDonald, 2023

Figure 6.2: Wave rose plots at Fa1, Fa2 Fa3, Fa4 and Fa5 for Hs (m) against MWD (deg.N) (a1-a5) and Tp (s) against MWD (deg.N) (b1-b5) for the 'Layout 01' conditions.



Source: Mott MacDonald, 2023

7 Summary

- Suitable bathymetric, wave, water level and wind data datasets were identified, quality assured and used to build, calibrate and validate a regional-scale and local MIKE21 FMSW models;
- To represent wave propagation correctly from offshore to nearshore areas around Fair Isle, the regional MIKE21 FMSW model covers a wide area of Shetland Islands and all relevant coastal and offshore areas that influence the wave conditions;
- The regional MIKE21 FMSW model was calibrated and validated against historical wave data at Lerwick station. During normal wave conditions and storm events, the model calibration and validation conformed to robust wave model performance metrics (Williams and Esteves, 2017). On this basis, the regional model was judged to be suitable for defining offshore boundary conditions for the local wave model and was run to transform 42 years of offshore wave data to the project site;
- Extreme value analysis was performed on 42 years of results from the regional wave model to define the wave characteristics of 100%, 50%, 10%, and 1% AEP events and to provide boundary conditions for the local wave model simulations of extreme wave events;
- Annual wave climate conditions were simulated for 2018, where the highest wave height was predicted in the 42-year wave record;
- Wave conditions were assessed using AEP and annual wave results from the local wave model at five wave data extraction points (Fa1 to Fa5) for the baseline and 'Layout 01';
- Hs slightly decreased at Fa1, Fa2 and Fa3 for Layout 01 due to shelter behind the breakwater;
- High Tp values were predicted at Fa1, Fa2 and Fa3 in Layout 01 due to reflection and directional spreading;
- The local model showed that the dominant wave direction is northwest to the north at Fa4 and Fa5 for the baseline layout. At these locations, the breakwater provides no shelter. At Fa2 and Fa3, behind the existing breakwater, the dominant direction is southwest to the west. Due to wave reflection, Fa1 shares the same dominant wave direction as Fa4 and Fa5.
- The dominant wave direction for 'Layout 01' conditions varies slightly from the baseline case at Fa2 and Fa3. At these locations, waves from the north are marginally more dominant due to the shape of the proposed layout.

It should be noted that the local wave model was not calibrated; therefore, there will always be some uncertainty until model calibration is performed. Nevertheless, the present study provides a useful guide to the performance of Layout 01 concerning impacts on the local wave climate.

For design purposes, it is considered that wave conditions would be simulated more accurately using a model like MIKE3 Wave FM that includes more physically realistic representations of reflection, diffraction and wave-wave interactions.

Appendices

A.	Comparison of regional and local models	40
B.	Wave occurrence	41

A. Comparison of regional and local models

Figure A.1: Time series of Hs based on the regional and local results at Point 2.

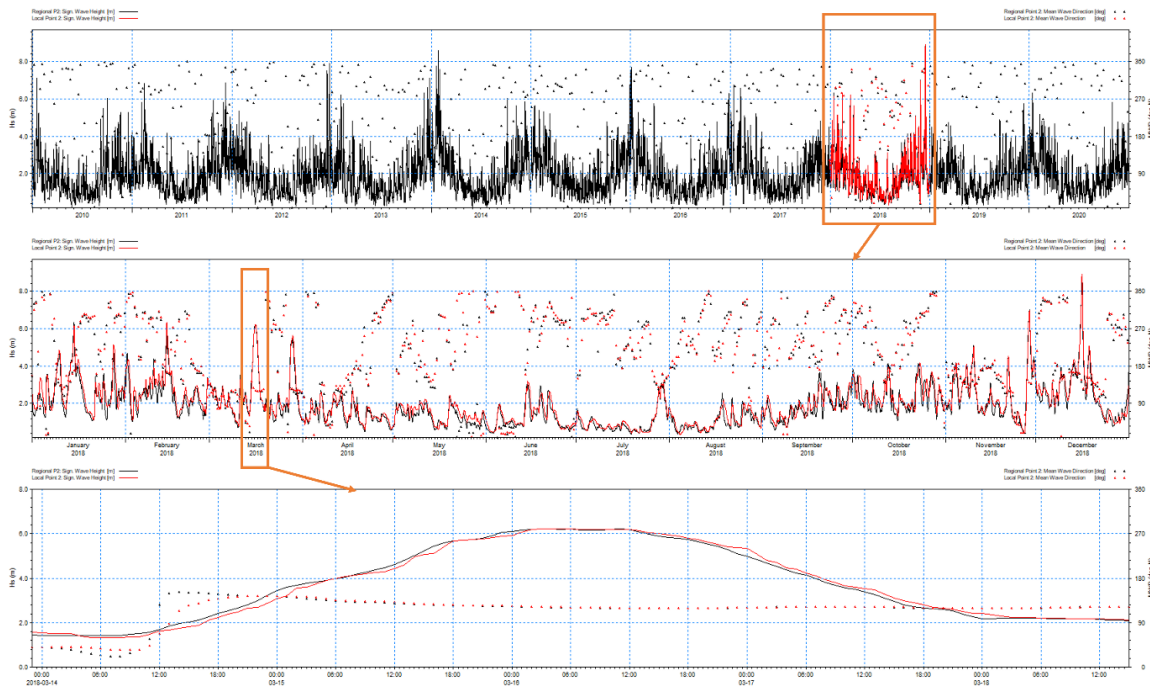
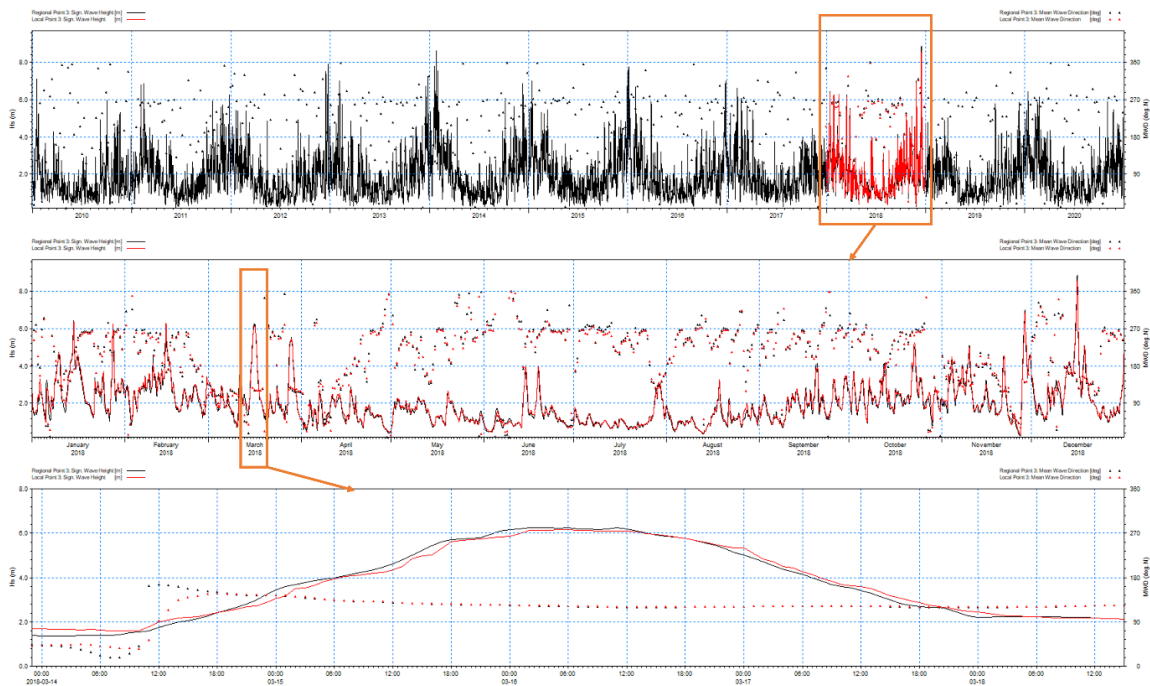


Figure A.2: Time series of Hs based on the regional and local results at Point 3.



B. Wave occurrence

B.1 Baseline

Table B.1: Annual wave occurrence of Hs (m) against Tp (s) at Fa1 for the baseline.

Hs (m) Tp (s)	0-0.1	0.1-0.2	0.2-0.3	0.3-0.4	0.4-0.5	0.5-0.6	Total	Total (%)
0-2	0	0	0	0	0	0	0	0
2-4	0	0	0	0	0	0	0	0
4-6	3	0	0	0	0	0	3	0
6-8	61	57	0	0	0	0	118	1
8-10	787	568	74	0	0	0	1429	16
10-12	1957	867	198	46	0	0	3068	35
12-14	1436	804	195	93	10	0	2538	29
14-16	479	495	113	24	0	0	1111	13
16-18	46	228	97	22	0	0	393	4
18-20	4	13	70	0	0	0	87	1
20-22	1	1	0	0	0	0	2	0
22-24	0	0	0	0	0	0	0	0
Total	4774	3033	747	185	10	0	8749	
Total (%)	54.6	34.7	8.5	2.1	0.1	0.0		100

Source Mott MacDonald, 2023

Table B.2: Annual wave occurrence of Hs (m) against Tp (s) at Fa2 for the baseline.

Hs (m) Tp (s)	0-0.1	0.1-0.2	0.2-0.3	0.3-0.4	0.4-0.5	0.5-0.6	Total	Total (%)
0-2	0	0	0	0	0	0	0	0
2-4	0	2	0	0	0	0	2	0
4-6	3	0	0	0	0	0	3	0
6-8	127	0	0	0	0	0	127	1
8-10	1297	121	0	0	0	0	1418	17
10-12	2748	277	2	0	0	0	3027	36
12-14	2067	311	28	0	0	0	2406	28
14-16	870	158	8	0	0	0	1036	12
16-18	205	154	6	0	0	0	365	4
18-20	15	70	0	0	0	0	85	1
20-22	1	0	0	0	0	0	1	0
22-24	0	0	0	0	0	0	0	0
Total	7333	1093	44	0	0	0	8470	
Total (%)	86.6	12.9	0.5	0.0	0.0	0.0		100

Source Mott MacDonald, 2023

Table B.3: Annual wave occurrence of Hs (m) against Tp (s) at Fa4 for the baseline.

Hs (m) Tp (s)	0-0.1	0.1-0.2	0.2-0.3	0.3-0.4	0.4-0.5	0.5-0.6	0.6-0.7	0.7-0.8	0.8-0.9	0.9-1.0	1.0-1.1	1.1-1.2	1.2-1.3	1.3-1.4	1.4-1.5	1.5-1.6	1.6-1.7	1.7-1.8	Total	Total (%)
0-2	0	0	0	0	0	0	0	0	0	0	0	0	0	0	0	0	0	0	0	0
2-4	0	0	0	0	0	0	0	0	0	0	0	0	0	0	0	0	0	0	0	0
4-6	0	0	0	0	0	0	0	0	0	0	0	0	0	0	0	0	0	0	0	0
6-8	107	53	32	51	12	4	10	0	0	0	0	0	0	0	0	0	0	0	269	3
8-10	535	295	234	246	151	161	71	19	7	4	4	7	0	0	0	0	0	0	1734	20
10-12	780	759	510	420	252	190	96	76	40	19	17	33	17	2	0	0	0	0	3211	37
12-14	91	513	397	172	258	206	155	72	67	40	25	27	34	16	3	7	1	0	2084	24
14-16	0	46	237	166	197	129	65	94	30	14	17	3	3	13	7	0	0	0	1021	12
16-18	0	0	0	32	45	50	81	80	15	26	6	4	3	2	7	6	0	0	357	4
18-20	0	0	0	0	0	2	7	22	35	14	16	13	0	0	0	0	0	0	109	1
20-22	0	0	0	0	0	0	0	0	0	0	0	0	0	0	0	0	0	0	0	0
22-24	0	0	0	0	0	0	0	0	0	0	0	0	0	0	0	0	0	0	0	0
Total	1513	1666	1410	1087	915	742	485	363	194	117	85	87	57	33	17	13	1	0	8785	
Total (%)	17.2	19.0	16.1	12.4	10.4	8.4	5.5	4.1	2.2	1.3	1.0	1.0	0.6	0.4	0.2	0.1	0.0	0.0		100

Source Mott MacDonald, 2023

Table B.4: Annual wave occurrence of Hs (m) against Tp (s) at Fa5 for the baseline.

Hs (m) Tp (s)	0-0.1	0.1-0.2	0.2-0.3	0.3-0.4	0.4-0.5	0.5-0.6	0.6-0.7	0.7-0.8	0.8-0.9	0.9-1.0	1.0-1.1	1.1-1.2	1.2-1.3	1.3-1.4	1.4-1.5	1.5-1.6	1.6-1.7	1.7-1.8	1.8-1.9	Total	Total (%)	
0-2	0	0	0	0	0	0	0	0	0	0	0	0	0	0	0	0	0	0	0	0	0	0
2-4	0	0	0	0	0	0	0	0	0	0	0	0	0	0	0	0	0	0	0	0	0	0
4-6	0	0	0	0	0	0	0	0	0	0	0	0	0	0	0	0	0	0	0	0	0	0
6-8	116	70	32	56	18	1	8	0	0	0	0	0	0	0	0	0	0	0	0	0	301	3
8-10	447	279	231	283	152	174	102	34	18	5	4	7	2	0	0	0	0	0	0	0	1738	20
10-12	599	742	455	564	265	205	126	101	31	28	26	20	32	7	3	0	0	0	0	0	3204	36
12-14	37	367	436	229	229	190	172	118	93	41	41	27	21	31	25	3	5	4	0	0	2069	24
14-16	0	6	98	231	135	179	118	57	77	34	19	11	16	2	13	6	0	0	0	0	1002	11
16-18	0	0	0	1	33	34	49	62	76	35	18	19	5	2	2	3	14	0	0	0	353	4
18-20	0	0	0	0	0	0	0	4	7	35	31	17	8	15	1	0	0	0	0	0	118	1
20-22	0	0	0	0	0	0	0	0	0	0	0	0	0	0	0	0	0	0	0	0	0	0
22-24	0	0	0	0	0	0	0	0	0	0	0	0	0	0	0	0	0	0	0	0	0	0
Total	1199	1464	1252	1364	832	783	575	376	302	178	139	101	84	57	44	12	19	4	0	0	8785	
Total (%)	13.6	16.7	14.3	15.5	9.5	8.9	6.5	4.3	3.4	2.0	1.6	1.1	1.0	0.6	0.5	0.1	0.2	0.0	0.0			100

Source Mott MacDonald, 2023

B.2 Layout 01

Table B.5: Annual wave occurrence of Hs (m) against Tp (s) at Fa1 for the ‘Layout 01’.

Hs (m) Tp (s)	0-0.1	0.1-0.2	0.2-0.3	0.3-0.4	0.4-0.5	0.5-0.6	0.6-0.7	Total	Total (%)
0-2	0	0	0	0	0	0	0	0	0
2-4	0	4	0	0	0	0	0	4	0
4-6	0	1	0	0	0	0	0	1	0
6-8	68	13	0	0	0	0	0	81	1
8-10	821	502	142	0	0	0	0	1465	17
10-12	1906	938	381	110	6	0	0	3341	38
12-14	1108	683	345	107	67	11	0	2321	27
14-16	244	553	204	15	17	0	0	1033	12
16-18	0	128	211	27	13	0	0	379	4
18-20	0	11	44	33	0	0	0	88	1
20-22	0	0	0	0	0	0	0	0	0
22-24	0	0	0	0	0	0	0	0	0
Total	4147	2833	1327	292	103	11	0	8713	
Total (%)	47.6	32.5	15.2	3.4	1.2	0.1	0.0		100

Source Mott MacDonald, 2023

Table B.6: Annual wave occurrence of Hs (m) against Tp (s) at Fa2 for the ‘Layout 01’.

Hs (m) Tp (s)	0-0.1	0.1-0.2	0.2-0.3	0.3-0.4	0.4-0.5	0.5-0.6	Total	Total (%)
0-2	0	0	0	0	0	0	0	0
2-4	7	5	0	0	0	0	12	0
4-6	8	0	0	0	0	0	8	0
6-8	84	0	0	0	0	0	84	1
8-10	1499	0	0	0	0	0	1499	20
10-12	2562	75	0	0	0	0	2637	34
12-14	1831	140	0	0	0	0	1971	26
14-16	983	26	0	0	0	0	1009	13
16-18	349	27	0	0	0	0	376	5
18-20	85	3	0	0	0	0	88	1
20-22	0	0	0	0	0	0	0	0
22-24	0	0	0	0	0	0	0	0
Total	7408	276	0	0	0	0	7684	
Total (%)	96.4	3.6	0.0	0.0	0.0	0.0		100

Source Mott MacDonald, 2023

Table B.7: Annual wave occurrence of Hs (m) against Tp (s) at Fa4 for the 'Layout 01'.

Hs (m) Tp (s)	0-0.1	0.1-0.2	0.2-0.3	0.3-0.4	0.4-0.5	0.5-0.6	0.6-0.7	0.7-0.8	0.8-0.9	0.9-1.0	1.0-1.1	1.1-1.2	1.2-1.3	1.3-1.4	1.4-1.5	1.5-1.6	1.6-1.7	1.7-1.8	Total	Total (%)
0-2	0	0	0	0	0	0	0	0	0	0	0	0	0	0	0	0	0	0	0	0
2-4	0	0	0	0	0	0	0	0	0	0	0	0	0	0	0	0	0	0	0	0
4-6	0	0	0	0	0	0	0	0	0	0	0	0	0	0	0	0	0	0	0	0
6-8	41	35	8	16	26	0	0	0	0	0	0	0	0	0	0	0	0	0	126	1
8-10	338	371	257	232	147	116	41	14	5	3	0	0	0	0	0	0	0	0	1524	17
10-12	623	862	592	401	338	206	112	66	29	23	41	14	6	0	0	0	0	0	3313	38
12-14	113	481	482	227	214	235	189	72	55	30	42	41	28	3	4	4	0	0	2220	25
14-16	0	38	273	277	194	113	84	81	23	16	2	5	8	10	1	0	0	0	1125	13
16-18	0	0	1	26	58	68	89	85	22	15	3	5	4	4	8	0	0	0	388	4
18-20	0	0	0	0	0	7	8	15	25	17	17	0	0	0	0	0	0	0	89	1
20-22	0	0	0	0	0	0	0	0	0	0	0	0	0	0	0	0	0	0	0	0
22-24	0	0	0	0	0	0	0	0	0	0	0	0	0	0	0	0	0	0	0	0
Total	1115	1787	1613	1179	977	745	523	333	159	104	105	65	46	17	13	4	0	0	8785	
Total (%)	12.7	20.3	18.4	13.4	11.1	8.5	6.0	3.8	1.8	1.2	1.2	0.7	0.5	0.2	0.1	0.0	0.0	0.0		100

Source Mott MacDonald, 2023

Table B.8: Annual wave occurrence of Hs (m) against Tp (s) at Fa5 for the ‘Layout 01’.

Hs (m) Tp (s)	0-0.1	0.1-0.2	0.2-0.3	0.3-0.4	0.4-0.5	0.5-0.6	0.6-0.7	0.7-0.8	0.8-0.9	0.9-1.0	1.0-1.1	1.1-1.2	1.2-1.3	1.3-1.4	1.4-1.5	1.5-1.6	1.6-1.7	1.7-1.8	1.8-1.9	Total	Total (%)	
0-2	0	0	0	0	0	0	0	0	0	0	0	0	0	0	0	0	0	0	0	0	0	0
2-4	0	0	0	0	0	0	0	0	0	0	0	0	0	0	0	0	0	0	0	0	0	0
4-6	0	0	0	0	0	0	0	0	0	0	0	0	0	0	0	0	0	0	0	0	0	0
6-8	30	28	5	12	35	0	0	0	0	0	0	0	0	0	0	0	0	0	0	0	110	1
8-10	257	359	218	266	167	108	89	22	5	4	4	0	0	0	0	0	0	0	0	0	1499	17
10-12	426	843	656	477	342	231	153	107	37	33	28	24	21	5	0	0	0	0	0	0	3383	39
12-14	26	322	497	357	173	168	209	173	81	34	47	30	34	38	6	4	4	4	3	0	2206	25
14-16	0	2	94	302	180	206	99	59	76	35	29	7	3	10	7	4	0	0	0	0	1113	13
16-18	0	0	0	3	21	55	41	74	86	46	20	6	5	5	3	4	9	0	0	0	378	4
18-20	0	0	0	0	0	0	0	7	8	20	22	18	12	9	0	0	0	0	0	0	96	1
20-22	0	0	0	0	0	0	0	0	0	0	0	0	0	0	0	0	0	0	0	0	0	0
22-24	0	0	0	0	0	0	0	0	0	0	0	0	0	0	0	0	0	0	0	0	0	0
Total	739	1554	1470	1417	918	768	591	442	293	172	150	85	75	67	16	12	13	3	0	0	8785	
Total (%)	8.4	17.7	16.7	16.1	10.4	8.7	6.7	5.0	3.3	2.0	1.7	1.0	0.9	0.8	0.2	0.1	0.1	0.0	0.0	0.0		100

Source Mott MacDonald, 2023

